Experimental Investigation of Cross-flow Induced Vibrations in a Tube Bundle using Wind Tunnel

By

Muhammad Adnan Rashid

2011-MS-MET-10

Thesis Supervisor

Prof. Dr. Nasir Hayat

DEPARTMENT OF MECHANICAL ENGINEERING
UNIVERSITY OF ENGINEERING AND TECHNOLOGY
LAHORE, PAKISTAN

2017

ABSTRACT

Flow induced vibrations in heat exchangers and steam generators is one of the critical problems the present industry is facing over past few decades. It is of major concern for designers, process engineers and operators, as it results in mechanical damage in the form of tube fretting wear, baffle damage, tube collision damage, tube joint leakage, tube failure due to fatigue or creep etc. Experimental investigations of cross flow induced vibrations in a tube bundle are carried out in this research work. Vibration behaviour of a single tube in a tube bundle has been examined by subjecting it to cross flow of air in a subsonic wind tunnel. The tube bundle consists of seven PVC tubes with 17.3 mm outer diameter arranged in rotated triangular configuration and has a pitch to diameter (P/D) ratio of 1.44. Tests are conducted in the wind tunnel over a range of free stream, air flow velocity from 3 to 20 m/s for which Reynolds number ranges from $0.34 \times 10^4 \leq Re \leq 2.29 \times 10^4$. The target tube is instrumented with strain gauges to measure the amplitude response in flow and lateral directions for each value of the upstream velocity.

The analysis shows that amplitude of the monitored tube in the lateral (Y) direction is larger than that of the flow (X) direction due to configuration of the tube bundle. It is also observed that vibration amplitudes of the monitored tube remain small in low velocity range which occurs due to turbulence in the upstream flow, caused by surrounding tubes. Vibration amplitudes increase significantly as the flow velocity is extended ahead of a threshold velocity which indicates the onset of fluid elastic instability. The threshold velocity for fluid elastic instability to occur, also known as critical velocity is 14 m/s in the current experiment. The stability map confirms that tube bundle is unstable in the current range of velocities and fluid elastic instability is inevitable. It is established that the occurrence of fluid elastic instability can be avoided by either keeping the cross flow velocities below the critical velocity or by controlling the damping ratio of the tubes.

Keywords: Cross flow, flow induced vibrations, tube bundle, P/D, rotated triangular, shell and tube heat exchanger, PVC tube.

DECLARATION

I certify that the research work titled "*Experimental Investigations of Cross-flow Induced Vibrations in a Tube Bundle using Wind Tunnel*" is my own work. The work has not been presented elsewhere for assessment. Where material has been used from other sources, it has been properly acknowledged / referred.

Muhammad Adnan Rashid
2011-MS-MET-10

ACKNOWLEDGEMENTS

*To begin with the name of **Almighty Allah**, the most Beneficent and Merciful, Who bestowed me with the courage and knowledge to complete this study.*

I would like to express sincere gratitude to my supervisor Prof. Dr. Nasir Hayat for his scholarly guidance, valuable suggestions and kind advice for completion of this research.

I also acknowledge and appreciate Prof. Dr. Shahab Khushnood (UET Taxila) for his valuable guidance and support throughout this research work. My special thanks to Mr. Luqman Ahmad Nizam (HITEC University) for his outstanding help and sparing his valuable time in completing the experimental work.

I am also thankful to my kind and loving parents, who supported me at each and every step of my research work and guided me with the best of their understanding.

TABLE OF CONTENTS

LIST OF FIGURES

LIST OF TABLES

NOMENCLATURE

English Symbols:

C_D	Drag force coefficient
C_m	Added Mass Coefficient
C_s	Side force coefficient
F_D	Drag force (N/m)
F_S	Side force (N/m)
U_∞	Free stream flow velocity (m/s)
U_p	Pitch/gap velocity (m/s)
U_r	Reduced velocity
V_c	Critical velocity (m/s)
V_{pc}	Critical pitch velocity (m/s)
d_i	Inner diameter of tube (mm)
d_o	Outer diameter of tube (mm)
d_{oe}	Equivalent tube diameter (mm)
d_{oe}/d_o	Equivalent diameter ratio
f_{an}	Natural frequency of Acoustic modes (Hz)
f_e	Excitation frequency (Hz)
f_n	Natural frequency (Hz)
f_{vs}	Vortex shedding frequency (Hz)
l_s	Tube span length (m)
m_h	Hydrodynamic mass per unit length (kg/m)
m_a	Mass of the fluid inside tube (kg/m)
m_i	Mass of the fluid inside tube per unit length (kg/m)
m_t	Total mass per unit length of tube (kg/m)

m_{tube}	Original mass of tube per unit length (kg/m)
A	Cross sectional area of tube (m^2)
C	Torsional stiffness (N/m)
D	Shell diameter (mm)
E	Modulus of elasticity (N/m^2)
I	Moment of inertia (m^4)
L	Tube length (m)
X_L	Longitudinal pitch to diameter ratio
X_T	Transverse pitch to diameter ratio
P/D	Pitch to diameter ratio
Q	Flow rate (liters/sec)
Re	Reynolds number
St	Strouhal number
K	Instability constant
T	Time period (sec)
$a(n)$	Fourier transform coefficient
g	Acceleration due to gravity (m/s^2)
n	Mode number
r	Radius of tube (mm)
P	Pitch of tube bundle (mm)

Greek Symbols:

λ_n	Frequency factor
ρ_{tube}	Density of tube material (kg/m^3)
ρ_a	Density of air (kg/m^3)
δ	Logarithmic decrement
ζ	Damping ratio

Abbreviations:

CFD	Computational fluid dynamics
FFT	Fast Fourier Transform
FIV	Flow induced vibrations
LES	Large Eddy simulations
PSD	Power spectral density
$TEMA$	Tubular Exchangers Manufacturers Association

Units:

Hz	Hertz
N	Newton
kg	Kilogram
m	Meter
m/s	Meters per second
mm	Millimeters
sec	Seconds

CHAPTER 1: INTRODUCTION AND OBJECTIVES

1.1 Introduction

Vibration problems occurring in different components of industrial plants are mostly due to fluid flow through these components. These vibrations problems impede smooth operation of industrial plants. Such flow related vibrations are known as flow induced vibrations. This has become a major concern in process, nuclear, petrochemical and power generation industries as it has caused failure of various industrial components in the past few decades. Such failure of critical components usually led to costly repairs and plant shutdowns.

Shell and tube heat exchangers are commonly utilized heat transfer equipment in process and power generation industries. Bundles of tubes are used in these heat exchangers whose function is to facilitate transfer of heat between two streams of fluids. One of the two fluid streams flows through the tubes while the other flows in the shell across the tubes outer side, to have an effective heat transfer between them. Tubes in the tube bundle of these heat exchangers are normally the most sensitive components of the assembly due to which they vibrate with varied intensity when subjected to cross-flow of shell side fluid. Excessive vibrations cause tube failure due to fatigue, fretting wear at the supports and damage due to tube to tube collision. General trend in designing heat exchangers is to utilize narrowly packed, thinner tubes with fewer supports and higher shell side velocities to increase the overall heat transfer coefficient and to decrease the shell side pressure drop and fouling. Unfortunately, these design practices tend to make tube bundles more susceptible to flow induced vibrations.

Failure of tubes of heat exchangers due to flow induced vibrations is costly because it results in expensive repairs and even plant shutdowns in addition to potential safety hazards. The danger of radiation exposure in case of component failure in heat transfer equipment used in pressurized water reactor (PWR) plants, requires extreme safety in designing. As a result of these problems, extensive theoretical and experimental research has been carried out on cross flow induced vibrations of heat exchangers tube bundles in past 30-40 years. Enormous literature has been developed as a result of this research and efforts are made to develop procedures and guidelines for failure prevention against flow induced vibrations.

Flow induced vibration in tube bundles subjected to cross flow is caused by different excitation mechanisms. The understanding and prediction of flow excitation mechanisms in tube bundles is vital for the safe design of heat exchangers. To date, it is generally agreed that there are four excitation mechanisms for tube vibrations in heat exchangers (Weaver, 1988).

- Turbulent buffeting
- Vortex shedding
- Fluid-elastic instability
- Acoustic resonance

The figure 1.1 presents the idealized response of a tube in a tube bundle subjected to cross flow showing different excitation mechanisms for tube bundle.

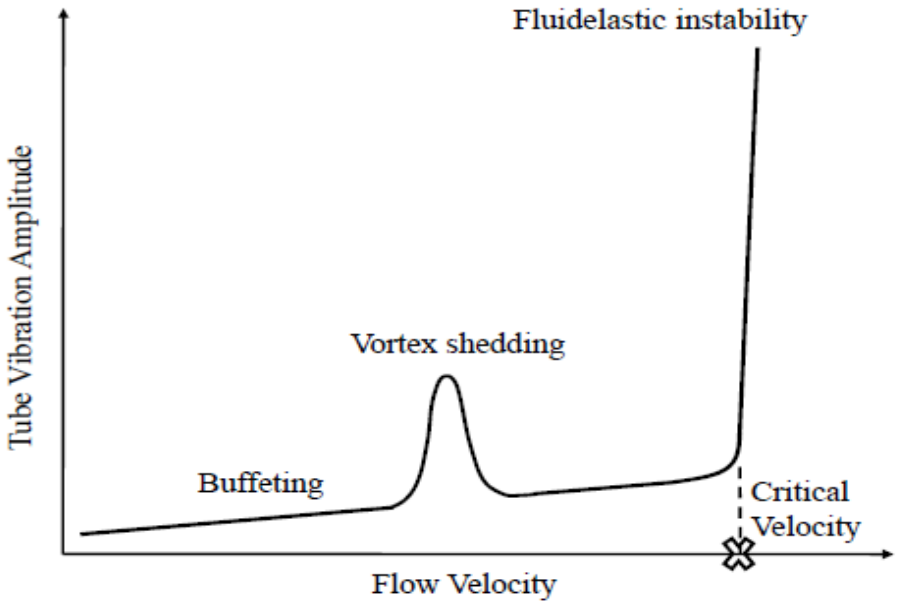

Figure 1.1: Idealized response of a tube bundle to cross flow (Paidoussis, 1981)

The progressive increase in vibration amplitude of tube with the increase in flow velocity is due to turbulent buffeting which is a forced vibration mechanism. When the frequency at which vortices are separating from the wake of tube to downstream flow matches with the tube natural frequency, then resonance may take place. As a result, the tube starts vibrating with relatively larger vibration amplitudes and the mechanism being termed as vortex shedding. As the flow velocity exceeds further, the tube comes out of the resonance zone and the response amplitude decreases following the vibration trend due to turbulent buffeting. When the flow velocity approaches a certain critical velocity threshold at which fluidelastic instability initiates, a dramatic increase of the vibration amplitude takes place. Fluidelastic

instability being a self-excited mechanism occurs when energy input to the tube mass-damping system surpasses the energy dissipated by the system and this will take place only after the critical velocity threshold has been exceeded. Acoustic resonance is produced when some flow excitation frequency coincides with the natural frequency of the heat exchanger cavity and is significant only in cases where shell side fluid is gas.

1.2 Objectives

This research is based on the vibration analysis of tubes in the tube bundle of shell and tube heat exchanger. PVC tubes were used to make a tube bundle with rotated triangular (60˚) arrangement. An experiment is performed by mounting the tube bundle in sub-sonic wind tunnel and subjecting it to cross flow of air. Investigation of vibration effects at mid span of an instrumented tube of the tube bundle is carried out by varying the velocity of air in the wind tunnel. Amplitude response of the instrumented tube in flow and lateral directions is recorded for each valve of the upstream velocity using data acquisition system. Natural frequency, vibration amplitude, damping, stability behaviour and other parameters were determined by using the experimental data and then their analysis is carried out. Finally, experimental results are compared with already published data.

1.3 Organization of Thesis

The present research is divided into five chapters. Chapter 2 covers the literature review summarizing theoretical background, pervious study reviews and the research framework for last few decades. Chapter 3 describes experimental setup, equipment and the sensors used for data acquisition and the experimental procedure employed in the current research. Chapter 4 covers the results of the experiment and their detailed analysis. Chapter 5 contains the comparison of current experimental results with previous published results, conclusions of current study and the recommendations.

CHAPTER 2: LITERATURE REVIEW

Flow induced vibrations is a high concern area in the design of shell and tube heat exchangers being used in power generation, petrochemical and process industries. The vibrations produced by high velocity shell side fluid flow in shell and tube heat exchangers may cause leakage or even fracturing of tubes in the tube bundle. Such failure of tubes due to flow induced vibrations leads to expensive repair and plant shutdowns. To overcome these problems, researchers have carried out extensive research in this area.

As a consequence of flow induced vibrations, damage to the tubes of heat exchangers is caused by three ways. Firstly for the tubes fitted to the fixed tubesheet, vibrations cause a circumferential crack at the tube root. Secondly at the location of baffle plates where tubes are loosely supported, low amplitude vibrations may cause failure of tubes due to fretting and impact wear. Thirdly in case of larger unsupported span of tubes, large amplitude vibrations may cause collision between the adjacent tubes.

Flow-induced vibration in a structure is caused by four mechanisms. Turbulent buffeting is identified by relatively small amplitude random vibrations produced as a result of external turbulent flow. Turbulent buffeting is not avoidable in heat exchangers since some level of turbulence is always present in shell side flow. Although turbulence in heat exchangers is desirable for enhanced heat transfer, the small amplitude vibrations due to turbulent buffeting may cause long term fretting wear at tube supports. Vortex shedding or Strouhal periodicity is the periodic separation of vortices alternatively from either side of the cylinder in a regular pattern when subjected to cross flow. As vortices detach from the cylinder, periodic pressure variations in flow field occurs. This gives rise to oscillating lift and drag forces which in turn causes periodic movement of the cylinder. Frequency of this periodic excitation increases with the increase in cross-flow velocity.

Fluid elastic instability is the exponential increase in vibrational amplitude of the heat exchanger tubes as a critical flow velocity is surpassed. This occurs when the energy input to tubes by the fluid forces dominate the energy dissipated by damping and in this way sufficient energy is transmitted to the tubes to uphold the vibrations. These resulting high amplitude vibrations can cause tube failures in a comparatively short period of time. Acoustic resonance refers to the development of an acoustic standing wave within the heat exchanger

shell which can cause loud sound emissions and large pressure fluctuations on the surrounding surfaces leading to structural damage.

2.1 Tube Layout Patterns

Four standard types of tube layout patterns are used in shell and tube heat exchangers: normal triangular (30°), rotated triangular (60°), normal square (90°) and rotated square (45°) as shown in Figure 2.1. These different tube layouts patterns can be arranged in decreasing order of shell side pressure drop and heat transfer coefficient as 30°, 45°, 60°, and 90° for identical tube pitch and flow rates. Thus, the 90° normal square layout will have the lowest pressure drop and heat transfer coefficient. The selection of suitable tube layout configuration depends on the following parameters:

- Compactness
- Rate of Heat transfer
- Pressure drop
- Accessibility for mechanical cleaning
- Phase change (if any) on the shell side

A tube bundle is an assembly of tubes, baffles, tubesheets, spacers and tie-rods. Spacers and tie-rods are used to maintain space between the baffles.

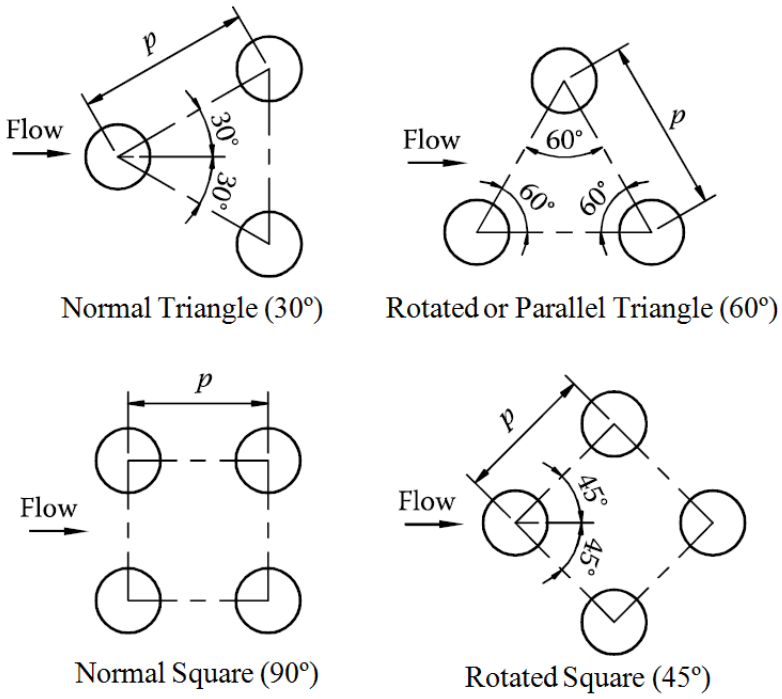

Figure 2.1: Different tube layout configurations

2.2 Excitation Mechanisms

As mentioned above, there are generally four excitation mechanisms in tube bundles. These four mechanisms are liable for most of tube failure in tube bundles including collision damage, wear damage, leakage, fatigue, creep etc.

2.2.1 Fluid Elastic Instability

Fluid elastic instability is a self-excited vibration mechanism and has the highest potential for damage to heat exchanger tube bundles in relatively short period of time. In self-excited vibration, the fluid force is a function of structural displacement. Physically, it is a problem of stability and is responsible for most short term tube failures (Paidoussis, 1981). Comprehensive reviews regarding this excitation mechanism have been given by Pettigrew et al. 1978, Paidoussis 1982 and Weaver & Fitzpatrick 1988. The instability can cause violent tube oscillation. Most severe damage is associated with fretting wear at the tube support plates or even tube to tube clashing in the U-bends. Due to the fact of its being a self-excitation mechanism, the amplitude of the vibration will continue to grow with increasing flow velocity after a critical instability velocity is exceeded.

Fluid elastic instability arises when the energy input to tubes by the fluid forces dominate the energy dissipated in damping and in this way adequate energy is transmitted to the tube to uphold the vibrations and an unstable situation is reached when the tube starts vibrating with large amplitude. At and above the critical flow velocity, a feedback mechanism exists between the vibrating tubes and the surrounding fluid such that energy from the flow is continuously transferred to the tubes. As a result, the amplitude of vibration increases exponentially to unacceptable levels. Typically, the design approach is to keep the natural frequency of tube arrays high enough, so that the working cross flow velocity is well below the critical velocity. However, this approach may result in over conservative designs of heat exchangers at the expense of thermal efficiency and higher capital cost. Extensive theoretical and experimental research has been conducted to obtain a better knowledge of the excitation mechanism and to find methods to correctly predict the threshold velocity.

2.2.1.1 Fluid-Elastic Instability Models

There are several theoretical models for fluid elastic instability that have been developed over the last few decades by different researchers. Few of them are described below (Price, 1995).

a. Jet Switch Model

A study on flow induced instability in tube bundles of heat exchanger was first made by Roberts (1966) who investigated both a single and a double row of cylinders normal to the flow. In preliminary experiments, Roberts found that instability occur only in the flow direction, with adjacent cylinders moving out-of-phase with each other. So, he limited his analysis to in-flow motion. On the basis of photographic evidence, Roberts represented the downstream flow of two nearby cylinders by two wake regions, one small and other large with a jet flow among them as shown in Figure 2.1.

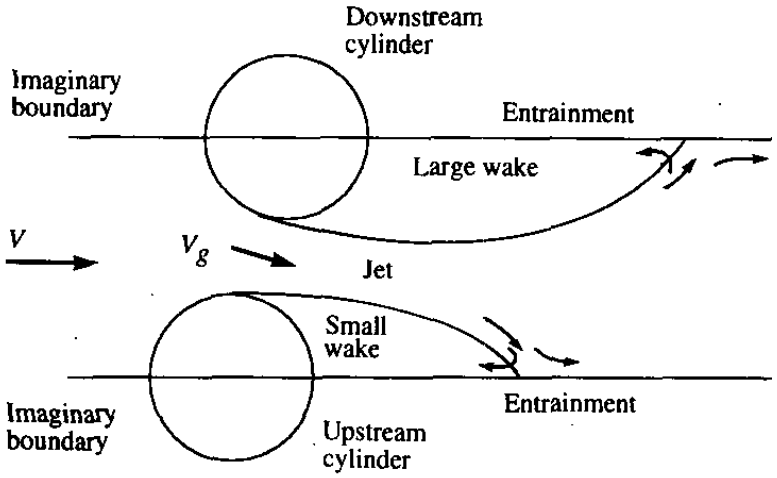

Figure 2.2: Jet-flow between two cylinders, Roberts jet switch model (1966)

Because motion was allowed only in flow direction, Roberts suggested that a hypothetical channel-flow involving two half cylinders and imaginary boundaries, as shown in Figure 2.1, was representative of the flow through a row of cylinders. Roberts considered it as a jet issuing close to a parallel flat plate with two wake regions supplied from the two sides of the spreading jet. The other main contribution of Roberts was that he accounted for the unsteady nature of the fluid flow. He realized that jet-reversal would not happen instantaneously, a finite time was required for the wake to diminish and the jet to change directions. Roberts suggested that jet-reversal will occur only if the time required is less than half the period of cylinder motion. Considering all these parameters, Roberts presented the following equation for occurrence of instability in a cylinder subjected to cross flow.

$$\frac{V_c}{\omega_n \epsilon D} = K\left(\frac{m\delta}{\rho D^2}\right)^{0.5} \tag{2.1}$$

Where ρ the fluid density and ε is the ratio of fluid elastic frequency to structural frequency, which is approximately equal to 1. This equation is very useful to predict the stability boundary of the vibrating cylinder. Figure 2.2 presents the Roberts experimental data with P/D =1.5, which was found supporting his theoretical model.

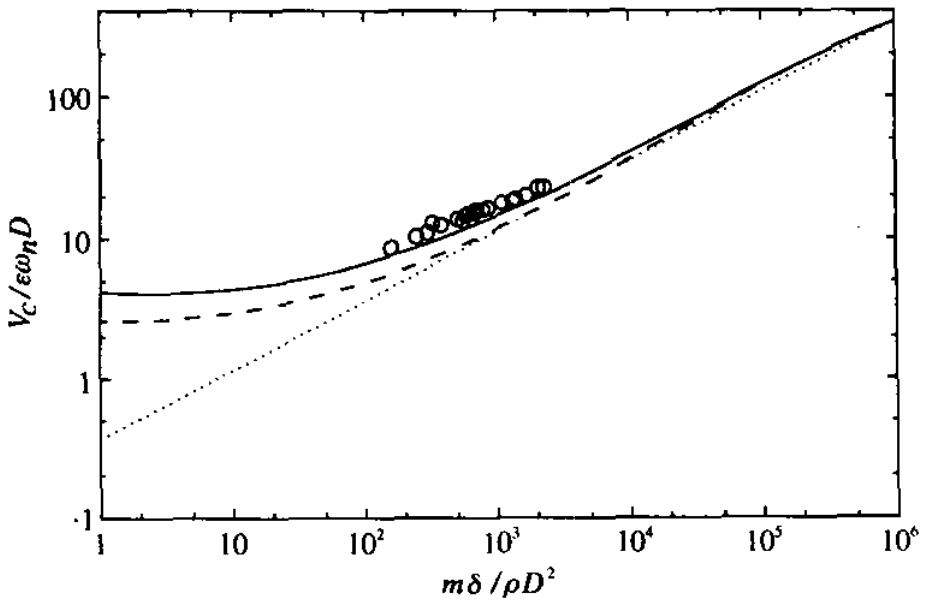

Figure 2.3: Fluid elastic instability, theoretical boundary for a single flexile cylinder in a row of cylinders (Roberts, 1966)

Applicability of Roberts' model is limited as cylinder motion is assumed to be effectively in the direction of flow by Roberts whereas most of experimental results reveal that predominate cylinder motion is in the direction normal to flow. Also, Roberts solution is applicable only for flexible single cylinder, whereas most of experimental data is for flexible multiple cylinders.

b. Quasi-static Model

Most famous expression predicting fluid elastic instability for cylinder arrays subjected to cross flow was originally developed by Connors (1970) and later by Blevins (1974) by using a quasi-static analysis. Similarly to Roberts, Connors and Blevins also considered a single row of cylinders normal to the flow. Instead of predicting fluid forces, Connors (1970) measured them experimentally. He found that tubes were predominantly vibrating in elliptical orbits in either in-flow or cross-flow directions. Connors carried out energy balances in both lateral and longitudinal flow directions using measured fluid stiffness. He devised a simple

stability criteria based on the quasi-steady theory and formulated the following relation for critical velocity beyond which large amplitude vibrations initiate.

$$\frac{V_{pc}}{f_n D} = K\left(\frac{m\delta}{\rho D^2}\right)^b \tag{2.2}$$

Where K is the instability constant also known as Connors coefficient, b is an exponent, $m\delta/\rho D^2$ is the mass damping parameter, f_n is the natural frequency, D is the cylinder outer diameter and V_{pc} is the critical pitch velocity which is defined as

$$V_{pc} = \frac{U_\infty P}{P - D} \tag{2.3}$$

K and *b* are coefficients obtained by fitting experimental data. Connors found values of 9.9 and 0.5 for *K* and *b* respectively from his experiments. Later on Connors suggested value of K = 2.7 – 3.9 for cylinder arrays (Connors 1978). Value of these constants is considered to be dependent on array geometry and fluid characteristics. Equation 2.2 developed by Connors is still frequently used for predicting results of fluid elastic instability. It correlates the two non-dimensional groups: reduced velocity and the mass damping parameter.

Equation 2.2 was re-derived by Blevins (1974) by considering that the fluid forces on a cylinder are caused by relative displacement between itself and its adjacent cylinders. Later on, Blevins (1979) reworked his analysis to include the flow dependent fluid damping and results in equation

$$\frac{V_{pc}}{f_n D} = K\left[\frac{m}{\rho D^2}\, 2\pi\left(\zeta_x \zeta_y\right)^{0.5}\right]^{0.5} \tag{2.4}$$

Where ζ_x and $\zeta_y$are total damping factors in the flow and lateral directions.

Pettigrew and Taylor (1991) suggested a value 3.0 for Connors coefficient in Equation (2.2) for all four standard tube array geometries (triangular, rotated triangular, square and rotated square), while ASME (2009) suggested a value of 2.4. Figure 2.4 shows a stability map reproduced from the ASME Boiler & Pressure Vessel Code (2009) which has collection of experimental data for all four standard array geometries. The current design approach involves fitting the Connors equation (Equation 2.2) to this experimental data to get an equation which predicts the minimum critical velocity for all the four standard array geometries in a conservative manner.

There are also many other models developed by different researchers over the past many years. These models include inviscid model, semi-analytical model, unsteady models, Computational fluid dynamics (CFD) models etc. Description of these different theoretical models has been summarized by Price (1995) in his work on fluid elastic instability.

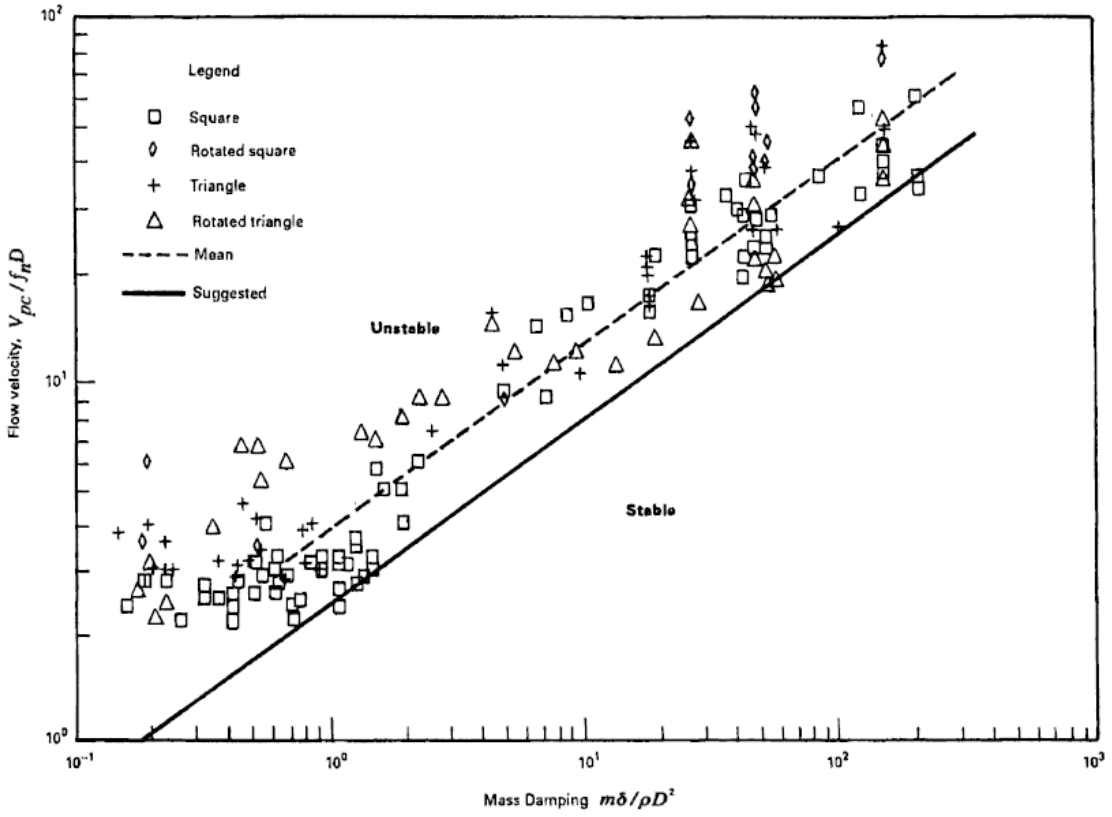

Figure 2.4: Fluidelastic stability diagram, ASME Boiler & Pressure Vessel Code (2009), Suggested stability threshold (solid line) corresponds to Equation (2.2) with K = 2.4 and the mean value (dashed line) corresponds to K = 4.0.

2.2.1.2 Recent Research on Fluid-Elastic Instability Phenomena

There are a number of different parameters which influence the occurrence of fluid elastic instability like tubes pitch ratio, tube bundle geometry, turbulence level, relative motion of surrounding tubes, type of working fluid, etc. As a result, study of fluid elastic instability involves all these different parameters which cause complexity. Researchers have developed an approach of examining a single flexible tube in a rigid tube bundle to study fluid elastic instability.

Austermann and Popp (1995) carried out experimental investigations of fluidelastic instability in different tube arrays subjected to cross flow of air in wind tunnel. They

investigated the consequence of pitch to diameter ratio on stability of tube bundles. They show that the stability of the tube arrays is also influenced by the position of flexible tube and tube array pattern. Rottmann and Popp (2003) performed wind tunnel tests on rotated triangular tube bundles with various flexible tubes to investigate their stability behaviour under different magnitudes of upstream turbulence. It was observed that upstream turbulence has a stabilizing effect on the tube bundles.

Mureithi et al. (2005) explored stability behaviour of a rotated triangular tube bundle in detail. Tests were conducted in wind tunnel by making different tubes to be flexible only in the flow direction. Reduced fluidelastic stability is observed as a result of increased flexibility in the tube array. On comparison with previous tests on unrestrained fully flexible arrays, critical velocity was found to be of same order of magnitude. On other hand, a single flexible tube in otherwise rigid bundle is observed to be stable.

Mitra et al. (2009) carried out experimental study of fluid elastic instability of horizontal tubes in single phase air flow and two phase steam water and air water cross flows. Tube bundles having normal square configuration with tubes made up of brass, stainless steel and aluminium were tested in wind tunnel and water tunnel separately. It was observed that instability occurs in both single phase and two phase flows and the critical velocity for initiation of instability was proportional to tube mass. A single flexile tube with rigid surrounded tubes is found to be more stable as compared to fully flexible tube bundles at lower flow velocities. Also tubes were found to be more balanced in steam water flow than air water flow.

Khalifa et al. (2012) performed experiment on all four standard types of tube bundle layouts to study their stability response. Experiments were executed in wind tunnel by using a single flexile tube in an otherwise rigid tube bundle and also by using fully flexile tube bundles. It was observed that fluidelastic stability behavior is significantly affected by tube location inside the bundle when it is tested as a single flexible tube in otherwise rigid bundle. It was also concluded that both damping and stiffness mechanisms are responsible for instability in tube bundles.

A summary of some recent research conducted by different researchers worldwide on the investigation of fluid-elastic instability in tube bundles of steam generators and heat exchangers is given in Table 2.1.

Table 2.1: Summary of some recent efforts carried out by researchers in fluid-elastic instability analysis

Researchers	Flow (Phase)	Analysis type	Frequency	Model type	Remarks
Khalifa et al., 2012	Single phase	Experimental, Wind tunnel testing, $P/D = 1.54$	20 Hz	Full flexible bundle and also a single flexible tube in rigid bundle, (Rotated triangular bundle)	Effect of tube flexibility and location inside the bundle on stability behaviour considered
Hassan et al., 2011	Single phase	Simulation (linear/non-linear) $P/D = 1.35$	90 Hz	Multi-span tubes with loose supports (Normal Triangular bundle)	Simulation of response of multi-span tube bundle with loose supports is carried out and compared with previous fluid force, time domain models
Sim & Park, 2010	Two phase (Air-water flow)	Experimental, Wind tunnel testing, $P/D = 1.3$	12-13 Hz	Flexible cantilevered cylinders (Normal square configuration)	Dependence of two phase damping on void fraction and effect of added mass and structural damping on dynamic instability is considered
Mitra at el., 2009	Single phase & two phase (Air-steam & Air-water flow)	Experimental, $P/D = 1.4$	7.5 - 13.3 Hz	Full flexible tube bundle and also a single flexible tube in rigid bundle (Normal square array)	Effect of tube mass and tube surface nucleate boiling on fluid elastic instability is examined
Mahon & Meskell, 2009	Single phase	Experimental, Wind tunnel testing, $P/D = 1.32, 1.58$	6.6 Hz	Normal Triangular bundle	Effect of time delay between flow field and tube motion on array stability is considered

Hassan & Hayder, 2008	Single phase	Modeling and simulation (Linear/Non-linear)	60 Hz	Time domain modeling of fluid forces on tubes	Critical velocity dependence on tubes pitch and turbulence level of flow is considered
Chung & Chu, 2006	Two phase (Air water cross flow)	Experimental $P/D = 1.633$	21-22 Hz	Normal & Rotated square arrays	Hydrodynamic coupling effect on stability and dependence of damping ratio on the void fraction considered
Mureithi et al., 2005	Single phase	Experimental, Wind tunnel testing $P/D = 1.37$	18-19 Hz	Multiple flexible tubes in cantilevered rigid array, Rotated triangular configuration	Investigations of response of tubes flexibility in flow direction and AVB's on stability behavior is carried out
Sasakawa et al., 2005	Two phase (Air water cross flow)	Experimental $P/D = 1.45$	30 Hz	Square array	Effect of void fraction fluctuations and flow patterns on fluid elastic vibration is considered
Rottmann and Popp, 2003	Single phase	Experimental, Wind tunnel testing, $P/D = 1.375$	8-9 Hz	Mutiple flexible cylinders in rigid array, Rotated triangular bundle	Analysis of effect of magnitudes of upstream turbulence on stability of cylinder arrays carried out
Austermann & Popp, 1995	Single phase	Experimental, Wind tunnel testing, $P/D = 1.25$	9.42 Hz	Single flexible cylinder in rigid array, all configurations	Effect of pitch to diameter ratio and position of flexible tube on stability of tube bundles considered

2.2.2 Vortex Shedding

When fluid flows across a cylinder, vortices are generated at the downstream of the cylinder (wake region) at certain flow velocity and separate periodically from either side of the cylinder as shown in figure 2.5. This periodic separation of vortices alternatively from either side of the cylinder in a cyclic manner causes periodic pressure variations in flow field. This result in oscillating lift and drag forces which may cause periodic movement of the cylinder. This phenomenon occurs more repeatedly as the velocity of the flow increases and is known as vortex shedding. Periodic shedding of vortices in the wake region is occurring at a dominant frequency which is called vortex shedding frequency, f_{vs}. The vortex shedding frequency is defined in terms of dimensionless Strouhal Number, St as

$$f_{vs} = \frac{St\ U_\infty}{d_o} \tag{2.5}$$

where U_∞ is the free stream velocity and d_o is cylinder outer diameter. At a certain valve of the free stream velocity, vortex shedding frequency matches with the natural frequency of the structure. At this stage, resonance occurs which results in large amplification of the lift force leading to high amplitude vibration of the cylinder. This phenomenon is termed as lock-in. Meanwhile drag force on the cylindrical structure also increases. However, the magnitude of the fluctuating drag force is lesser than the fluctuating lift force. Also the drag force appears at twice the vortex shedding frequency. No significant vibration occurs unless the vortex shedding frequency matches the natural frequency of cylinder. This excitation mechanism is also referred as Strouhal periodicity, Strouhal excitation or periodic wake shedding.

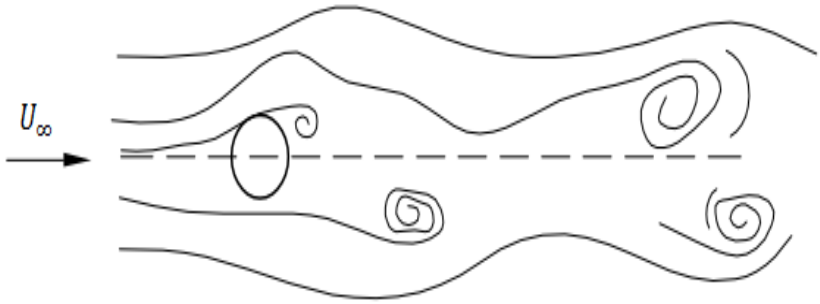

Figure 2.5: Vortex shedding for a single cylinder

Vortex shedding mechanism for a single cylinder is well understood and a number of researchers have investigated this phenomena. Chen and Weber (1970) reviewed variation of Strouhal number and lift and drag force coefficients over the entire range of Reynolds number being applied during experimentation. For cross flow across a single cylinder, the Strouhal number is nearly constant at 0.2 for a range of Reynolds number $300 \leq Re \leq 2 \times 10^5$. After this due to shortening of the wake region, the Strouhal number increases slowly. But the wakes become completely turbulent as the Reynolds number excels the value of 3.5×10^5. No regular vortex shedding occurs at this stage. This behaviour lasts up to a Reynolds number of 3.5×10^6. After surpassing this value, a Von Karman vortex can be formed again and Strouhal number is about 0.27 in this range.

For the case of two cylinders in cross flow that are positioned in close proximity, the dynamical behaviour differs from the single cylinder case because the presence of additional cylinder and wake interference affects the overall flow field. Location of the flow separation points on the cylinder surface depends on cylinders configuration, their natural frequencies and pitch-to-diameter (*P/D*) ratio. In the case of a strong coupling between the cylinders, vibrations in both lateral and longitudinal directions may occur. When the vortex shedding frequency matches the cylinder natural frequency then resonance occurs. This leads to lock-in and hence results in large amplitude vibrations of the upstream cylinder. Several studies have been carried out for vortex shedding phenomena of cylinder pairs in different configurations; tandem, side-by-side, staggered etc. A comprehensive review has been presented by Zdravkovich (1977).

Occurrence of vortex shedding phenomena in multiple cylinders or tube arrays subjected to cross flow was traditionally considered to be similar to that of a single isolated cylinder. Past experimental and numerical work shows that vortex shedding produces a resonance peak similar to that observed for isolated cylinders for certain tube array geometries in water flows and a clear resonant peak does not occur for most of tube array geometries especially in gas flows (Weaver and Fitzpatrick 1988). This occurs because damping is generally sufficient in gas flows to suppress large amplitude vibrations. Typical vortex shedding in a tube array is shown in Figure 2.6, X_L and X_T are lateral and longitudinal pitch respectively.

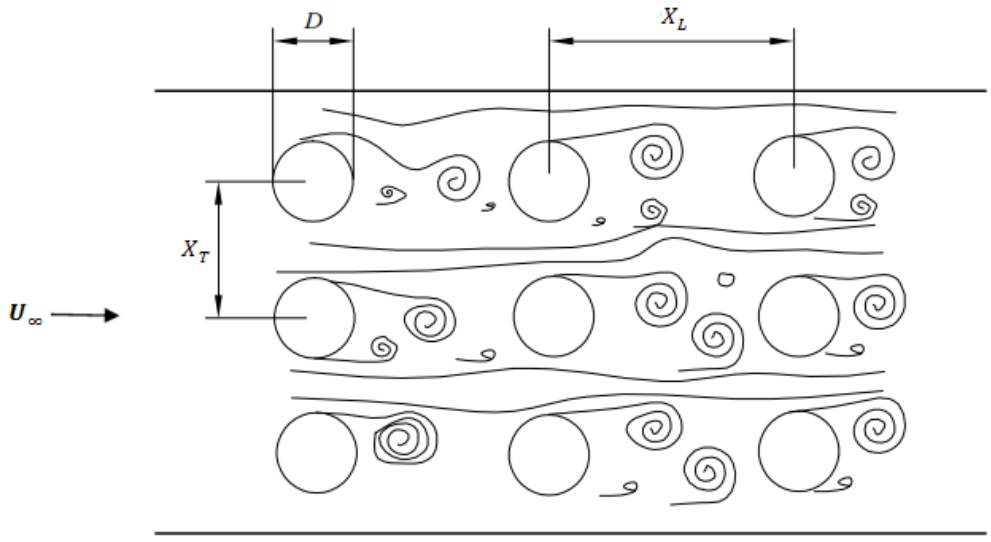

Figure 2.6: Vortex shedding in a tube bundle

Vortex shedding excitation has been recognized since 1950's but the possibility of formation of vortices inside closely spaced tube bundles has been disputed by Owen (1975). According to him, coherent vortices could not form deep in the array due to small space between the tubes and high levels of turbulence. He argued that the observed periodicity within the array is rather due to resonance of dominant turbulent buffeting frequency in turbulent flow field with the natural frequency of the tube. Although his work did not receive wide acceptance, it highlighted the need for an alternate, more elaborate model than the classic Karman vortex shedding model (Paidoussis 1982). As a consequence, Chen (1977) proposed numerous mechanisms and portrayed different flow structure patterns which could cause vortex shedding excitation e.g. jet switch, wake swing and jet instability models. However, to date, experimental confirmation of those mechanisms and patterns could not be achieved.

Grover and Weaver (1978) found vortex shedding peaks at constant Strouhal number of 0.83 in the turbulence spectra of the flow deep inside a parallel triangular array. High amplitude vibrations due to occurrence of vortex shedding were observed only in initial tube rows of the under investigation tube array and no excessive vibration response was found after 15^{th} row. As vortex shedding occurred at very high Strouhal number so very low energy is available at tube resonance due to which the amplitude response also remain small. In addition, no lock-in between tubes natural frequency and shedding frequency is observed due to insignificant interaction of the tubes with the flow. As a result, dangerous vibrations due to vortex shedding had not occurred in the tube array.

Strouhal number is not constant for tube arrays; instead it changes with the layout configuration and spacing of tubes. Typical values for in-line and staggered tube bundle geometries have been presented in the form of design charts by Fitzhugh (1973) and Blevins (2001) as shown in Figure 2.7.

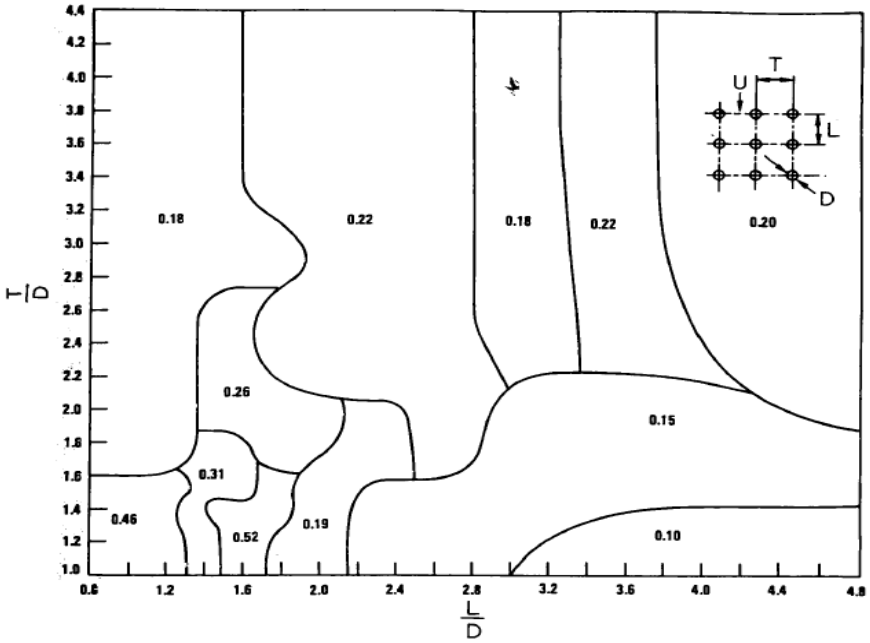

(a)

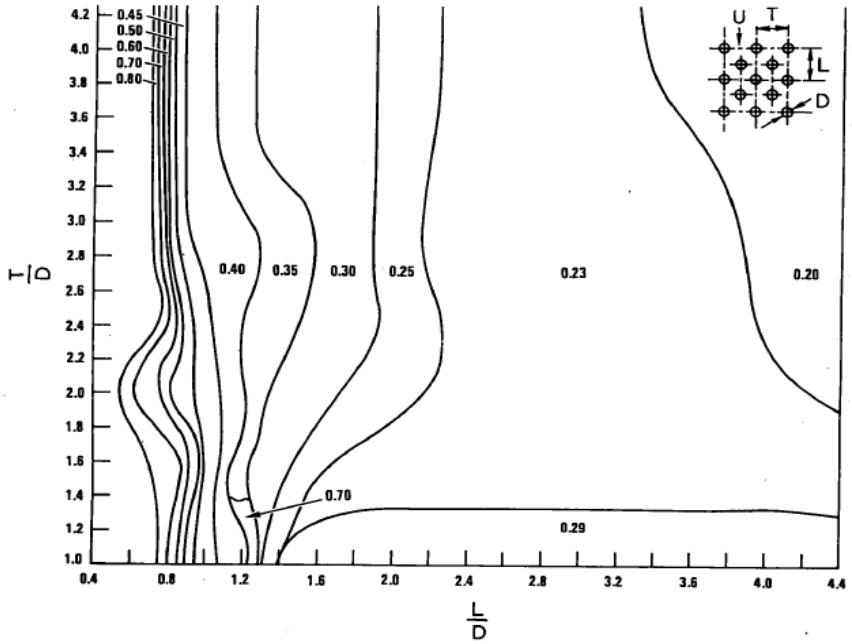

(b)

Figure 2.7: (a) Strouhal numbers for in-line tube arrays (b) Strouhal numbers for staggered tube arrays (Fitzhugh, 1973)

Ziada and Oengoren (1992) tested an in-line tube bundle in air and water flows to investigate the occurrence of the vortex shedding excitation and the associated flow structure. Vortex shedding excitation was observed to be caused by unstable fluid jet flowing through the gaps between the tubes. This unstable jet occurred at a specific mode and results in large size vortices on both sides of the flow lines. The measured results and the flow visualization images clearly depicted a developing flow pattern due to unstable jet in the initial few rows of the tube array.

Polak and Weaver (1995) experimentally tested normal triangular tube arrays in wind tunnel to study vortex shedding excitation mechanism. It was observed that structural or acoustic resonance had not occurred in the array, so no large amplitude vibrations were encountered. Hot wire measurements were used to measure the intensity, spatial and temporal correlations of the flow fluctuations and the results had been supported by flow visualization. The constant Strouhal number phenomenon observed was due to alternate shedding of vortices from the few initial tube rows. It was observed from experimentation that the Strouhal number depends upon Reynolds number, location of measurements in the array and pitch ratio of the array. The study provided a consistent set of data and guidance for estimating the Strouhal numbers for normal triangular arrays over the entire range of practical pitch ratios.

Pettigrew and Taylor (2003) outlined and discussed vortex shedding mechanism in addition to other flow induced vibration excitation mechanism in heat exchangers. Methods for prediction of vibration response and design guidelines for prevention of periodic wave shedding are also discussed. It was concluded that there are a number of parameters which effect the magnitude of fluctuating forces due to vortex shedding like bundle geometry, location in the bundle, turbulence, Reynolds number, pitch to diameter ratio and density of fluid.

Williamson and Govardhan (2008) have outlined and discussed the theoretical studies and experimental work done related to vortex induced vibrations in the last two decades, with special emphasis on energy transfer and vortex dynamics mechanisms that results in different modes of vibrations. They highlighted the significance of mass damping and the concepts of effective elasticity, critical mass and the relationship of force with vorticity in addition to other points. From forced vibration studies, new modes for vortex wake have been compiled in the framework map of vortex modes. It was also established that some of these modes of vortex wake cause free vibration.

Liang et al. (2009) studied numerically the impact of spacing between tubes on the characteristics of vortex shedding and varying forces in an inline tube array subjected to laminar flow at a Reynolds number of 100. The study involved computational analysis of a six-row inline tube array for eight different pitch to diameter ratios ranging from 2.1 to 4, using Navier–Stokes and continuity equations based code. Rms lift and drag coefficients and mean drag was found to become maximum for the spacing range of 3.0 to 3.6. With the increase in spacing between tubes, flow became more unsymmetric and vortex shedding started to induce from the last cylinder and proceeded upstream. The instantaneous streamline pattern for larger spacing depicted that there was phase difference of 180º between two successive cylinders as shown in figure 2.8 and during one shedding period, vortices traveled a distance nearly equal to twice of the tube spacing.

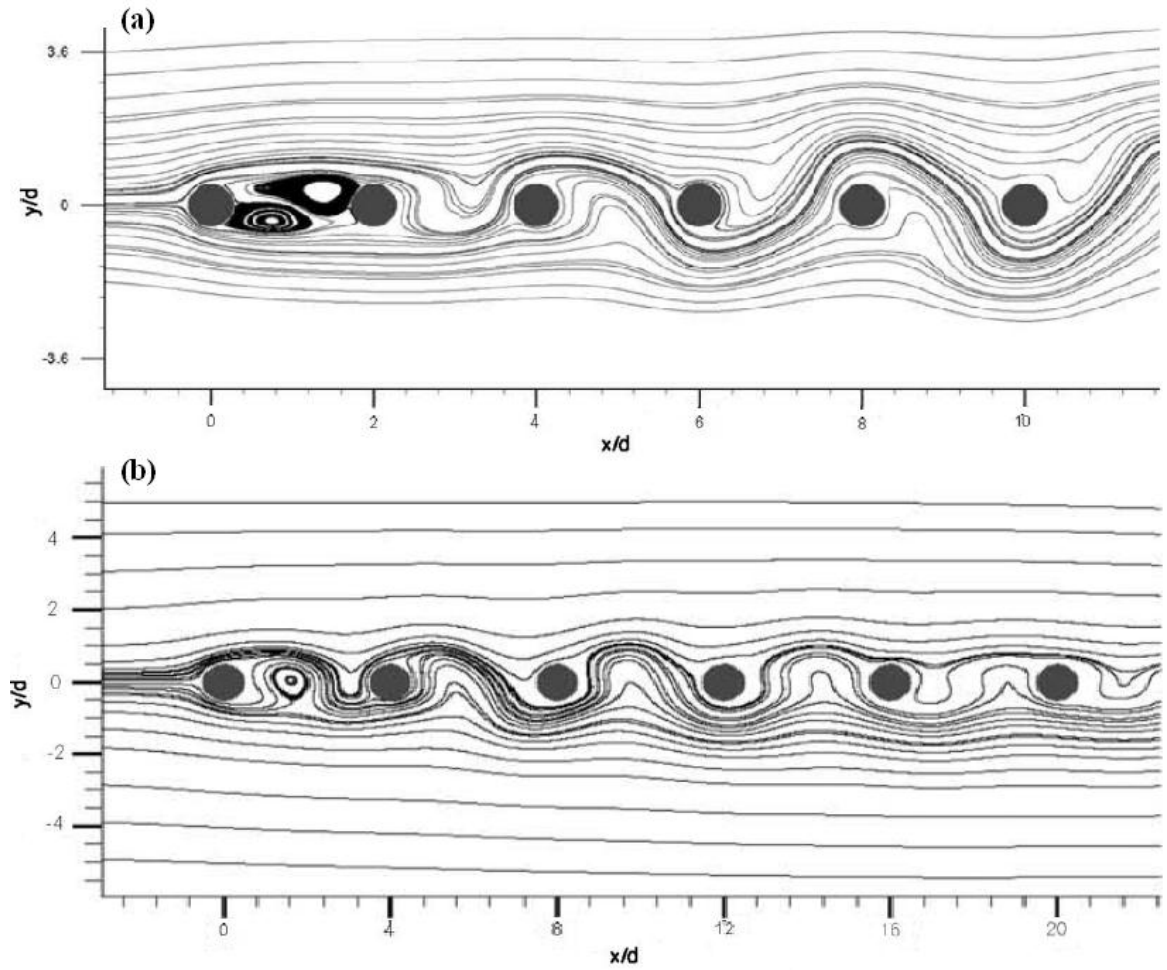

Figure 2.8: Instantaneous response of in line tube array: (a) P/D = 3.6 (b) P/D = 3.4 (Liang et al., 2009)

Hamakawa et al. (2011) performed wind tunnel testing of normal triangular tube arrays with closely mounted serrated fins to study characteristics of vortex shedding phenomena. Significant vortex shedding was observed over the applied range of Reynolds number within the finned tube arrays and also in the wake of the arrays, with Strouhal numbers of 0.20 and 0.40. It was revealed that the Strouhal number calculated using measured values of pitch velocity and vortex shedding frequency in the wake of array agreed closely with that obtained from Fitzhugh's map for staggered tube arrays.

2.2.3 Turbulence Excitation

Turbulent buffeting is a forced vibration mechanism and is associated with the development of unsteady forces in the body exposed to external turbulent flow which cause relatively small amplitude random vibrations. Turbulence in tube bundles subjected to cross flow increases as the fluid flows across the array geometry, as a consequence tubes are subjected to turbulent buffeting at all practical Reynolds numbers. Although turbulence in heat exchangers is desirable for enhanced heat transfer, the small amplitude vibrations due to turbulent buffeting may cause long term fretting wear at tube supports. So it is desirable to estimate buffeting response in the design phase to increase the effective life of the equipment.

Turbulent buffeting response normally occurs at velocities below the critical instability velocity and also away from the vortex shedding lock-in velocity region. Turbulent eddies in the shell side flow in heat exchangers are scattered around a central dominant frequency over a wide range of frequencies. A considerable amount of energy transfer occurs when the dominant turbulent buffeting frequency approaches the lowest natural frequency of the tube, which causes resonance and high amplitude vibration of the tube. If resonance does not occur even then turbulent buffeting can cause fatigue failure and fretting wear at tube supports. Due to requirement of extreme safety in the operation of nuclear power plant, relatively small tube wear rates in heat exchangers and steam generators cannot be acceptable.

Owen (1975) carried out detailed study to understand the characteristics of turbulence in tube bundles and suggested a semi-empirical model for approximation of peak dominant frequency in the turbulence frequency band. He attributed the noticed tube vibration and acoustic resonance phenomena to that dominant turbulent buffeting frequency in the broadband turbulence spectrum. It was later experimentally observed that the Owen’s model

is quite reliable provided that minimum pitch velocity is used (Weaver and Grover, 1978). The expression proposed by Owen for the peak turbulent buffeting frequency, f_{tb} is given as

$$f_{tb} = \frac{U_\infty}{DX_L X_T}\left[3.05\left(1-\frac{1}{X_T}\right)^2 + 0.28\right] \tag{2.6}$$

Where X_L is longitudinal pitch ratio, X_T is transverse pitch ratio and D is tube outer diameter. Owen's work did not receive wide recognition and was questioned by many researchers in later years. Weaver and Grover (1978) experimentally investigated turbulent buffeting mechanism in a rotated triangular array in wind tunnel. Experiments were performed at different flow velocities after the disappearance of vortex shedding phenomena up to the occurrence of fluid elastic instability threshold. Random tube response due to turbulent buffeting was observed in these tests and no periodic motion was noticed even when the turbulence spectrum peak matches with the tubes' natural frequency. Strength of turbulence spectrum peak was reliant on the geometry of tube array and the same may also cause acoustic resonance in tube arrays.

Oengoren & Ziada (1998) carried out experimental analysis of the mechanisms of turbulence excitation, vortex shedding and acoustical resonance in three normal triangular tube bundles with different pitch ratios separately in air and water single phase flows. Test were carried out up to Reynolds number range of 53000 and involve pressure, velocity and force measurements along with substantial visualization of the flow structure at resonant and non-resonant conditions. It was observed that with the increase in Reynolds number, turbulence level increase gradually. Determination of bound spectra for calculation of turbulent forces acting on the tubes was also worked out by the authors.

Pettigrew and Taylor (2003) reviewed and discussed turbulence excitation mechanism in addition to other flow induced vibration mechanism in tubular heat exchangers. According to them, turbulence generated within tube bundle was a source of random excitation in interior tubes of bundle whereas turbulence generated by inlet ports, nozzles and piping elements was responsible for random excitation of upstream tubes in case of single phase liquid flows. They considered random excitation due to turbulence not to be a serious problem for gaseous and vapour cross flows as the resulting excitation forces and pressure variations are less than those encountered for liquid and two phase cross flows. Authors have also developed design guidelines for random excitation forces in single and two phase flows in the graphical forms using data from different sources.

Paul et al. (2008) conducted experimental and numerical study of turbulent cross flow in a staggered tube array which has longitudinal and transverse pitch to diameter ratios of 2.1 and 3.8 respectively. Experiments were conducted in water tunnel at a Reynolds number of 9300. It was noticed that lateral turbulence intensity is considerably higher than the longitudinal turbulence intensity. Different theoretical models were used to forecast the turbulent flow. Numerical results from some theoretical models were found to be in close resemblance with the experimental results.

Placzek et al. (2009) performed numerical simulation of flow around a circular cylinder oscillating perpendicularly to the incoming stream with a fixed Reynolds number of 100. An industrial CFD code was used to determine cylinder displacement. Simulations have been performed with free and forced oscillations. Amplitude and frequency spectrum of the cylinder were investigated at different reduced velocities to observe different phenomena. The results suggested that vortex shedding modes are related to the frequency response and have shown a very good agreement with the other similar studies using different numerical approaches.

Endres & Moller (2009) performed experimental investigations of the transmission of a disturbance with fixed frequency generated by an obstacle, in the incident cross flow through a tube array with square configuration and its impact on the pressure and velocity variations inside the array. It was observed that increasing turbulence levels of the cross flow through the tube array in addition to external disturbance lead to rise in amplitude due to the resulting pressure variations on the surface of tubes in the array. Presence of peaks in velocity spectra due to disturbance in wake frequency was found up to 5th row. In the region between first and second row, measured spectra had values higher than the original disturbance which was due to increase in turbulence intensity. As the flow passes through the succeeding tubes rows, turbulence levels remains almost constant whereas the effect of disturbance diminishes.

Paula et al. (2012) have studied turbulence in triangular tube array by hot wire measurements in an aerodynamic channel and flow visualization in water channel. The tube arrays have P/D ratios of 1.26 and 1.6, and Reynolds number rangers from 7.5×10^{3} to 4.4×10^{4}. A stable wake pattern was observed after the first row of tubes for both P/D ratios. Visualization depicted that flow that arises from the gap between two tubes form coalescent jets. In some cases, changing flow direction occurs. The turbulence feature of flow after third, fourth and fifth row was observed to be similar.

2.2.4 Acoustic Resonance

Acoustic resonance is a self controlled excitation mechanism and refers to development of an acoustic standing wave within the heat exchanger shell which can cause loud sound emissions and large pressure fluctuations on the surrounding surfaces leading to structural damage. This typically happens when the vortex shedding frequency matches with a transverse acoustic natural frequency of the heat exchanger shell. The established acoustic standing waves are transverse to both the tube span and flow direction. This phenomenon is normally associated with gas flows as resonance is difficult to develop in liquid cross flows due to higher speed of sound and relatively lower flow velocities of liquid flows.

Acoustic standing waves caused by the acoustic resonance mostly produce an intense, low frequency, pure tone noise whose intensity may reach 175 dB sound pressure level. Such a considerably high sound pressure level can cause vibration and noise problems in heat exchangers. However, acoustic resonance does not necessarily occur even though the condition of frequency coincidence is satisfied as it also depends on the magnitudes of acoustic energy and acoustic damping. Natural frequency of the acoustic modes, f_{an} of the heat exchanger shell can be estimated by (Ziada et al., 1989):

$$f_{an} = \frac{nC}{2W} \tag{2.7}$$

Where W is the size of heat exchanger shell cavity in the direction normal to tube axis and flow, C is the speed of sound in shell side fluid and n is the mode order (number of the acoustical standing half waves along the dimension W). Transverse velocity fluctuations of acoustic standing waves with different mode orders are shown in figure 2.9. Acoustic resonance occurs when the natural frequency of any acoustical mode approaches the shedding frequency i.e.

$$f_{vs} \approx f_{an} \tag{2.8}$$

Common methods to avoid acoustic resonance in heat exchangers include either avoiding resonance by utilizing a flow velocity away from resonant zone or by installing one or more anti-resonant baffles in the tube array to suppress and distort the resonant acoustical waves. Reviews on acoustic resonance phenomena have been provided by Paidoussis (1982), Weaver and Fitzpatrick (1988) and Blevins (1984), who considered acoustic resonance in heat exchangers to be interlinked with vorticity excitation.

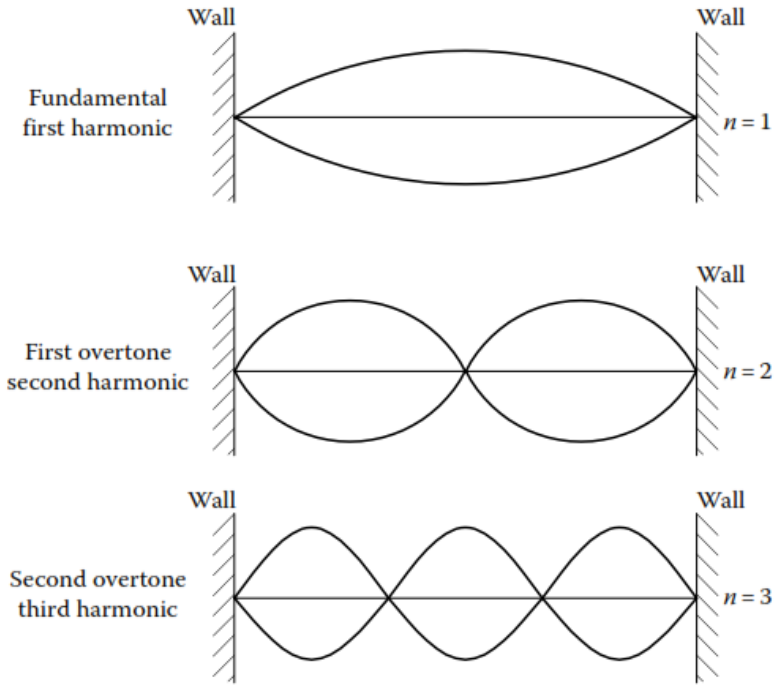

Figure 2.9: Transverse velocity fluctuations of acoustic standing waves with different mode orders

Ziada et al. (1989) experimentally investigated acoustic resonance phenomena in in-line and staggered tube arrays subjected to cross flow of air and water separately. The authors found that there are multiple Strouhal numbers at which periodicity occurred for each array are not harmonic of each other. Flow periodicities downstream of first row of tubes were noticeable which caused acoustical resonances. The authors attributed it to be the major source of excitation for acoustical resonance in closely packed tube arrays. At the incidence of frequency match, magnitude of Reynolds number was observed to have an important influence on the occurrence of acoustic resonance and its higher values make the system more susceptible to acoustic resonance.

Oengoren and Ziada (1992) studied acoustic resonance in an in-line configuration tube array by performing experiments in air and water flows. It was observed that flow instability pattern which caused acoustic resonances is quite different from the normal jet instability causing vortex shedding at constant Strouhal number. Acoustic resonance occurs due to the coupling between the acoustical resonant sound field and the unstable shearing fluid layers detaching from the tubes. The flow structures were found to be completely different for resonant and non-resonant states. Strouhal numbers for acoustic resonance were also found different from those of vortex shedding.

Feenstra et al. (2005) experimentally investigated the impact of acoustical noise on the amplitude of tube vibration in a staggered tube bundle and measured the efficiency of baffles in reducing the effect of transverse acoustic modes. Tube vibration induced by an acoustical standing wave inside the test duct was worked out for a flexible tube at three different lateral locations in the tube bundle. It was observed that the monitored tube vibrates with maximum amplitude when it was situated at the center of testing duct for the case of fundamental transverse acoustical mode because a nodal point exists at the center of duct. However, when the same tube was positioned near the duct side wall, it was not much influenced by the acoustical standing wave even though acoustic pressure oscillation was highest at that location. It was found that first mode of resonance was eliminated by inclusion of a single baffle plate in the test section, whereas only slight noise reduction was observed for the second and higher acoustical modes. The authors concluded that a single baffle cannot be entrusted to overcome all acoustic modes.

Eisinger and Sullivan (2007) studied acoustic resonance phenomena in an in-line tube array of boiler at full load flow and proposed solutions to suppress it. Strong acoustical resonance was observed in the lower portion of tube array with acoustic pressure reaching up to 165 dB and at an acoustical frequency of 132 Hz. Observed acoustic waves were considered to be of first transverse acoustic mode, caused by vortex shedding at resonance from the gas flowing across the tubes. Authors found that acoustical resonance can be restrained by an acoustical baffle positioned at the center of the flow passage in the affected portion of tube array.

Acoustical behaviour of two side by side cylinders subjected to cross flow of air was experimentally analyzed by Hanson et al. (2009). Six different P/D ratios in range of 1.25 to 3 were used for the cylinder pair to determine its effect on acoustic resonance mechanism. Bistable flow features caused by downstream wakes were observed for small to intermediate pitch ratios i.e. for $P/D < 2.2$. Acoustic resonance did not commence at either of the two observed Strouhal numbers for vortex shedding before the occurrence of resonance. Instead acoustic resonances occurred at a Strouhal number, which lies in between those observed in the bistable flow regime. It was concluded by the authors that in this case, acoustic resonance integrates with vortex shedding and eradicate bistable flow phenomena as shown in figure 2.10. Whereas, for large spacing ratios ($2.5 \leq P/D \leq 3.0$), vortex shedding was observed to occur at a single Strouhal number at which the acoustic resonance is excited.

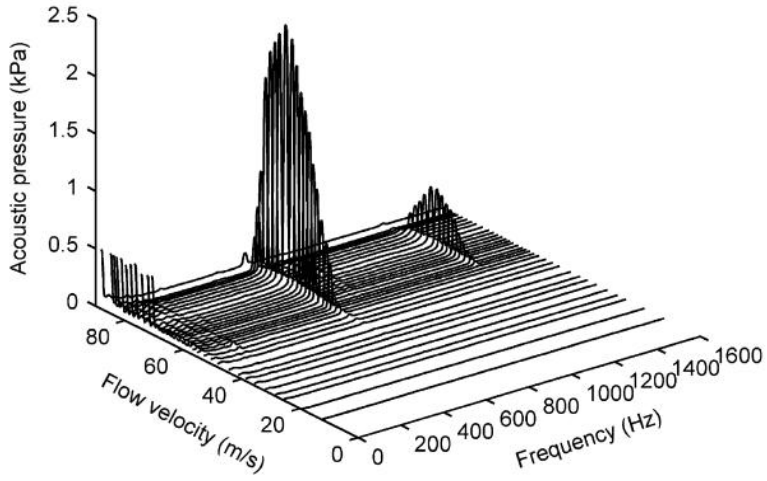

Figure 2.10: Acoustic pressure spectrum for two side by side cylinders for $P/D = 1.25$ over the whole flow velocity range (Hanson et al., 2009)

2.3 Natural Frequency of Tube Vibration

Tubes in the tube bundle are the most flexible components in a shell and tube heat exchanger and they may be modeled as slender beams. When the tubes are excited, they vibrate at different frequencies. The lowest frequency at which the tube vibrates is called natural frequency. Knowledge of natural frequency of tubes is important for flow induced vibration design of heat exchangers because resonant conditions can only be avoided by keeping the excitation frequencies away from the natural frequency of tubes.

Natural frequencies of straight and curved tubes having single or multiple spans can be determined by a number of different analytical and numerical techniques. These tubes may have different support conditions at the ends. Tubes are fixed to the tubesheet rigidly and supported along the span length at intermediate supports by support plates or baffles. Tubes near the center of the tube bundle are usually supported by every baffle present in between the tubesheets, whereas the tubes near the outer periphery of the tube bundle that pass through the baffle window may be supported at every second or third baffle. In the spans between baffles, amplitude of vibration of tubes remains unlimited as the tubes vibrate. Whereas, it is constrained to tube to baffle hole clearance at the location of baffles.

Natural frequency of tubes is influenced by a number of factors like geometry, span length, density and elastic properties of material, span shape, tube to support clearance, axial loading and type of support at end of span. Determination of natural frequency of the tube bundle by considering multi-span tube bundle as a whole, by using current state of the art vibration

analysis techniques is quite complex. Singh and Soler (1984) treated a tube as continuous elastic beam with ends fixed at the tube sheet and simply supported at intermediate points by the baffles. Then each individual span is considered as a separate beam with its own end conditions (pinned-pinned, fixed-pinned etc) as shown in figure 2.11.

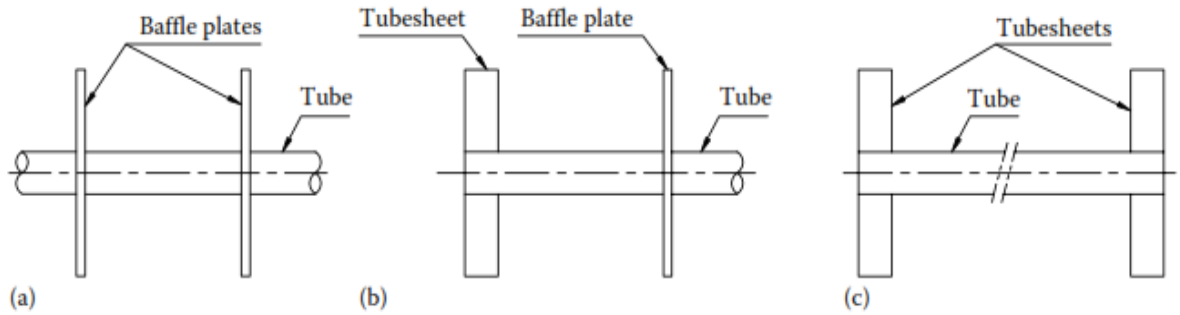

Figure 2.11: Individual span geometry with different end conditions (a) pinned-pinned (b) fixed-pinned (c) fixed-fixed

Natural frequencies are calculated for each individual span and then the lowest frequency is taken as the representative value for the complete tube and hence for the whole tube bundle. This method of determining natural frequency by considering individual spans separately is also recommended by Zukauskas (1989) and TEMA (2007). The general form of equation for natural frequency along with the effect of axial stress is given by

$$f_n = \frac{1}{2\pi} \frac{\chi_B \lambda_n}{l_i^2} \sqrt{\frac{E\,I}{m}} \tag{2.9}$$

Where E is the modulus of elasticity of the tube material, I is moment of inertia of the tube cross-section, m is effective mass of tube per unit length, l_i is the length of tube unsupported span between the supports and χ_B is the axial stress factor. The coefficient λ_n is called frequency constant and is a function of vibration mode, baffle spacing and end conditions. Values of λ_n for first mode and different end conditions are given in table 2.2. The axial stress factor for the tube unsupported span is given by

$$\chi_B = \sqrt{1 + \frac{F_a}{F_{cr}}} \tag{2.10}$$

In this equation, F_a is the tube axial load and F_{cr} is the critical bucking load.

Table 2.2: Values of Frequency Constant λ_n for Different End Conditions

End Conditions	Value for 1st Mode
Pinned-Pinned	9.87
Fixed-Pinned	15.42
Fixed-Fixed	22.37

2.4 Dynamic Parameters

Knowledge of added mass and damping is a vital requirement for vibration analysis of tubular heat exchangers. These dynamic parameters generally depend on fluid properties (in particular, fluid viscosity and density), geometry of the component and adjoining boundaries (whether rigid or elastic).

2.4.1 Added Mass

During flow induced vibration in a heat exchanger, vibration of tubes in the tube bundle causes displacement of shell side fluid which in turn produces a change in inertia of the fluid flowing around the tubes. This effect is known as added or hydrodynamic mass because it increases the apparent mass of the vibrating tubes. Added mass has a significant effect on the natural frequency of tubes. The impact of added mass on natural frequency is encountered by including it into apparent mass of the vibrating tube. Hydrodynamic or added mass is defined as the product of mass of the fluid dislocated by tube and an added mass coefficient 'C_m'.

$$m_h = C_m(\pi r^2 l)\rho$$

On per unit length basis, it becomes

$$\frac{m_h}{l} = C_m(\pi r^2)\rho \tag{2.11}$$

Where ρ is the density of the fluid, r is the tube outer radius and l is the tube length. Since hydrodynamic mass increases the total mass of the vibrating tube therefore it causes a decrease in the natural frequency of tube.

The added mass coefficient is determined either by analytical formula developed by Blevins (1990) or by using experimental data of Moretti et al. (1976). The analytical formula

developed by Blevins to find out added mass coefficient for a single flexible tube in a rigid array of tubes is given as

$$C_m = \frac{(d_{oe}/d_o)^2 + 1}{(d_{oe}/d_o)^2 - 1} \tag{2.12}$$

Where $d_{oe}/d_o = [0.96 + 0.5(P/D)](P/D)$, in which d_{oe} is the equivalent diameter of neighboring tubes and the ratio d_{oe}/d_o represents the confinement in tube array.

The experimental results of Moretti et al. (1976) for a single flexible tube in a rigid triangular or square array with pitch to diameter ratios in the range of 1.25 to 1.50 is shown in figure 2.12. TEMA has included this figure in their standards (TEMA Standards, 2007) for approximation of added mass coefficient.

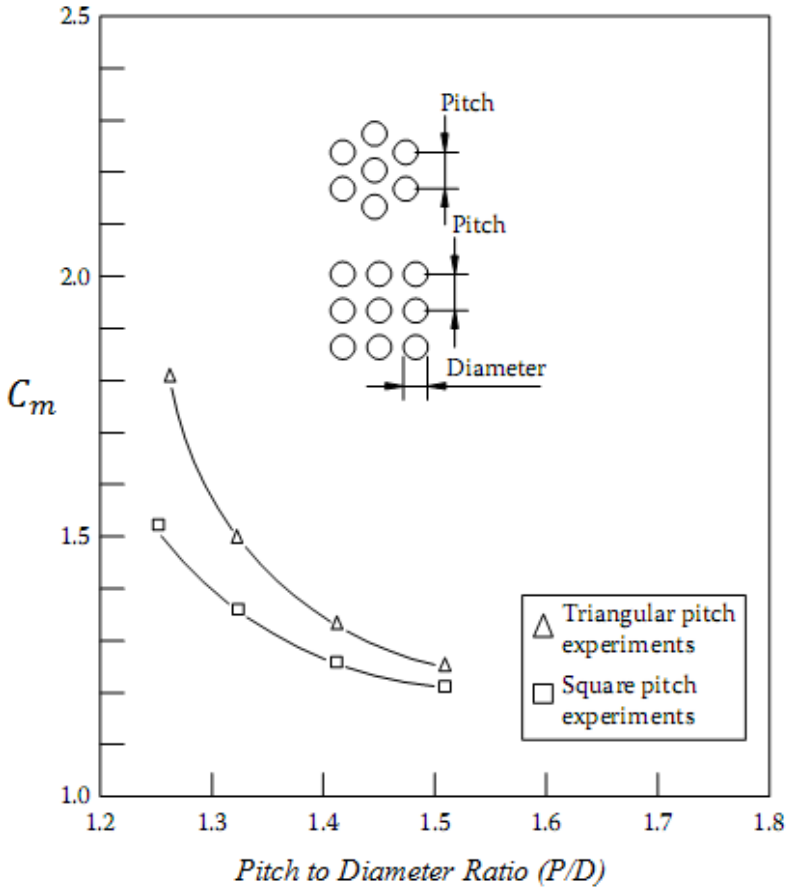

Figure 2.12: Experimental Data for Added Mass Coefficient (Moretti et al., 1976)

2.4.2 Damping

Damping is the process of energy dissipation of a vibrating system as a result of dissipative forces (friction, fluid resistance, internal forces etc). Damping causes decay of vibration in a

vibrating structure. It depends on geometry, material of structure, vibration frequency and physical properties of the surrounding fluid. Amount of damping in a system is expressed as damping ratio 'ζ' which is defined as the ratio of actual damping coefficient to critical damping coefficient of the system.

$$\zeta = \frac{c}{c_c} \tag{2.13}$$

Where actual damping coefficient 'c' and critical damping coefficient 'c_c' are characteristics of the system and have units newton-second per meter (*Ns/m*). The rate of decay of free vibration is quantified by taking natural logarithm of the ratio of any two consecutive amplitudes. This factor is known as logarithmic decrement 'δ' and is defined as

$$\delta = \ln\left(\frac{x_n}{x_{n+1}}\right) \tag{2.14}$$

It terms of damping ratio, it becomes

$$\delta = \frac{2\pi\zeta}{\sqrt{1-\zeta^2}} \tag{2.15}$$

When ζ is small, then $\sqrt{1-\zeta^2} \cong 1$. So the above expression becomes

$$\delta = 2\pi\zeta \tag{2.16}$$

In shell and tube heat exchangers, damping has a significant effect on the stability of the tube bundle. Damping restricts the response of a tube being excited by any excitation mechanism. It depends on the mechanical properties of tube, tube frequency, support characteristics and properties of the surrounding fluid. In most of the cases, the value of damping ratio varies from 0.01 to 0.17. Pettigrew et al. (1991) have outlined different mechanisms of energy dissipation that results in damping of tubes in a tube bundle which are presented in table 2.3.

Table 2.3: Energy Dissipation Mechanisms (Pettigrew et al., 1991)

Type of Damping	Source
Structural	Depends on tube material
Viscous	Depends on the fluid forces acting on the tube
Flow-dependent	Depends on the characteristics of fluid
Squeeze film	Depends on the fluid present between tube and support
Friction	Depends on the coulomb damping present at supports
Tube support	Depends on the characteristics of support material

Two-phase	Depends on the liquid gas mixture
Thermal	Depends on the temperature of fluids

Calculation of damping in tube bundles by using experimental methods is quite difficult. Different researchers have developed empirical formulas for estimation of damping for both gases and liquid flows on shell side. After reviewing available experimental data on damping of tubes in multi-span heat exchangers with gas flow on shell side, Pettigrew et al. (1986) formulated empirical correlations for calculation of damping ratio. They established that prominent damping mechanism in gas flows is friction between tubes and baffle supports. Therefore baffle thickness and number of baffle supports are the significant parameters contributing to damping in gas flow. Whereas, lateral clearance between the baffle supports and tubes has much less significance in damping.

Pettigrew et al. (1986) have also given recommendations for heat exchanger tube design in liquid flows. According to them, dominant damping mechanisms in liquid flows are tube to fluid viscous damping, friction damping at baffle support and squeeze film damping between baffle support and tube.

2.4.2.1 Parameters Influencing Damping

There are many types of parameters that influence damping, some of which are as follows:

a) **Type of tube motion:** The tube vibrates in two directions, rocking motion and lateral motion. Damping in the rocking motion of the tube is considerably less than the lateral motion.
b) **Effect of number of supports:** Damping in tubes is largely dependent on the supports material and characteristics. Larger the number of supports for the tube, higher is the damping in the tubes and vice versa.
c) **Effect of tube Frequency:** Damping has generally no relation with the frequency of vibrating tubes.
d) **Effect of vibration amplitude:** Also, the amplitude of vibration does not have a significant role in the damping of the tubes.
e) **Effect of diameter or mass:** Researches have shown that damping of tubes is independent of the tube diameter or mass.

f) **Effect of side loads:** In real heat exchangers, side loads are due to the fluid forces on the tubes. So, generally high side loads result in high energy dissipation and in turn cause high damping.

g) **Effect of tube support thickness:** Supports thickness is one of the major factors in the damping of the tubes. Thicker the support, higher is the damping in the tubes.

h) **Effect of clearance:** No significant trend in the damping data was reviewed for the normal range of tube-to-baffle support diametral clearances (0.40mm - 0.80mm).

2.5 Summary of Recent Studies in the Field of Flow Induced Vibrations

The summary of recent experimental studies carried out by different researchers in the field of flow induced vibrations is given in the table 2.4.

Table 2.4: Summary of recent experimental studies carried out by different researchers for analysis of flow induced vibrations

Name of Researcher	Experimental Setup	Conditions	Results
Duro, V., Decultot, D., Maze, G. (2011)	• Test section is of rectangular section of 6m, 4m and 3m (length, width and height respectively. • The accelerometer is installed to measure vibrations. • Air filled copper cylindrical tube of length=1.353 m is immersed in water.	• Reynolds number = 135000	• Tubes excited by the flow generate four vibration modes. • The analysis provides close results to the experimental results.
Lam, K., Lin, Y.F., Zou, L. (2010)	• Test section is of 2.1, 0.15 and 0.3 m (length, width and height) respectively. • Water in closed loop is used as a working fluid. • Free stream velocity was adjusted from 0 to 4m/s.	• Reynolds number ranges from 0 to 7500. • The turbulence intensity level in free stream is about 2%.	• The turbulence kinetic energy behind the first row of tube bank is reduced. • The power spectral density of vortex shedding in the tube bundle is suppressed.
Yahiaoui, T., Adjlout, L., Imine, O., (2010)	• Tube bundles consist of 7 rows with 40 mm outer diameter of tube. • Air is used as a working fluid. • It is driven by AC motor with the maximum velocity of 60m/s. • P/D = 1.44 (P = 57.6 mm, D = 40 mm).	• Reynolds number = 35500 • Free stream velocity (U_{∞}=3.1321 m/s) • Gap velocity (U_p=10.2505 m/s)	• Flow in inline tube bundles is observed to be unsymmetric and transient. • For all Reynolds number, the coefficient of drag decreases for tube 3 and tube 6.

Iqbal, Q., Khushnood, S. (2010)	• Test section consists of triangular (60˚) bundle with pitch of 15.875 mm and tube outer diameter of 12 mm. • The internal fluid of the tube is air and the shell fluid is water.	• Water (shell side fluid) temperature is varied from 30˚C to 90˚C.	• Natural frequency of the tubes varies with the increase in the temperature of water. • Damping also increases with rise in temperature.
Endres, L.A.M. and Moller, S. V. (2009)	• Rectangular channel of length, width and height *1370 mm*, *193 mm* and *146 mm* respectively. • Air is used as a working fluid. • P/D ratio=1.60 and 32.1 mm diameter of tubes and 5×4 tube bundles.	• For single cylinder, Re=20000 • For tube bank, Re=17000	• Results indicate that the frequency of the disturbance remains unaltered as it passes through the bank. • Flow velocity varies with the position.
Said, N.M., Mhiri, H., Bournot, H., Palec, G.L. (2008)	• Test section consists of rectangular channel of 3000 x 200 x 300 mm (length, width and height) respectively. • The axis of the tube bundles is perpendicular to the flow.	• Reynolds number ranges from 8500 to 64000. • The turbulence intensity level in free stream is about 0.2%.	• Flow pattern is based on the gap between the tubes. • A reasonable level of agreement is found between experimental and numerical data.
Paul, S.S., Ormiston, S.J., Tachie, M.F. (2008)	• Test section is of rectangular section is 2500, 200 and 200 mm (length, width and height) respectively. • Water in closed loop is used as a working fluid. • Bundle is of 6 rows of tubes with 25.4 mm outer diameter of tube.	• Reynolds number = 9300	• Results show that there is high turbulence generation by the normal stresses as well as regions of negative turbulence.

Olinto, C. R., Endres, M., and Moller, S. V. (2007)	• Test section consist of three tube banks having square arrangement with P/D = 1.26, 1.4 and 1.6 respectively.	• Reynolds number in the gap between tubes is found to be 70000 to 80000.	• Results show that there is presence of instability from the second row of tube bank. • This instability travels through the tube bundle till the last row of tubes.
Inada, F., Kawamura, K., Yasuo, A. (2002)	• Test section consist of square tube bundle having P/D = 1.42. • Tubes are subjected to air water two phase cross flow.	• Velocity of water varies from 0 to 6 m/s. • Air velocity varies from 0 to 7.5 m/s.	• Added mass, damping and stiffness is found to be the function of non-dimensional gap velocity and void fraction in two-phase flow. • Results also show that equivalent added mass and damping does not depend on the tube vibration amplitude. • Non-linearity starts appearing when the tube displacement reaches 4.5 mm.

CHAPTER 3: EXPERIMENTAL SETUP

3.1 Introduction

In the current research, PVC pipes are used to form a tube bundle. This tube bundle is then mounted in a sub-sonic wind tunnel and is subjected to cross flow of air. Cross flow induced vibrations in the tube bundle are analyzed by recording the vibration spectrum of the bundle. Natural frequency, damping and other parameters are determined and compared to the values computed numerically.

3.2 Experimental Setup

The experimental setup for the current research work consists of the following.

- The experiment is carried out in an open subsonic wind tunnel. The test section is made up of perspex glass and has a cross section of 292 x 292 mm^2 with a length of 450 mm. The maximum wind velocity is 20 m/s. The air flow is driven by an axial fan with speed controlled motor. A slanted tube manometer is utilized to measure the current air velocity at inlet to the test section which is also displayed on the data acquisition unit.
- A tube bundle made of PVC is used in the experiment. The tube bundle consists of seven tubes arranged in 60^o rotated triangular pattern according to the criteria defined by Blevins (Blevins, 2001). The specifications of the tube bundle are presented in the table 3.1.
- The tubes used in the tube bundle have an outer diameter of 17.3 mm and a span length of 281 mm. The ratio of the tube center to center spacing to tube diameter, P/D is 1.44. All the tubes are rigidly mounted in the acrylic end plates. The assembled tube bundle is shown in figure 3.2.
- The central tube of the bundle is instrumented with four 120 Ω strain gauges in full bridge (wheatstone bridge) configuration at mid-span to record vibration amplitude in the flow direction as shown in figure 3.1. After taking a complete set of reading in the flow direction, the target tube is rotated by 90^o to record the vibration amplitude in the lateral direction.
- Data acquisition system consists of SG-Link mXRS wireless sensing node (shown in figure 3.3 (a)) along with the WSDA-104 USB Base Station (shown in figure 3.3 (b))

connected with PC through Node Commander Software developed by MicroStrain Inc.

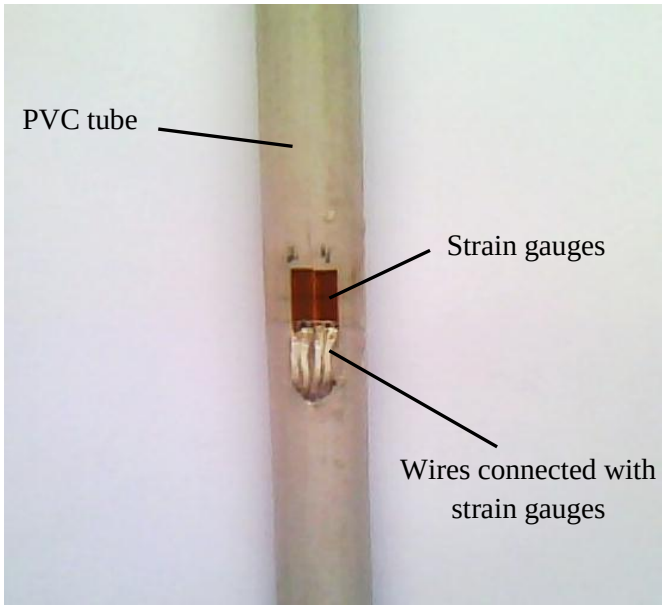

Figure 3.1: Instrumented tube

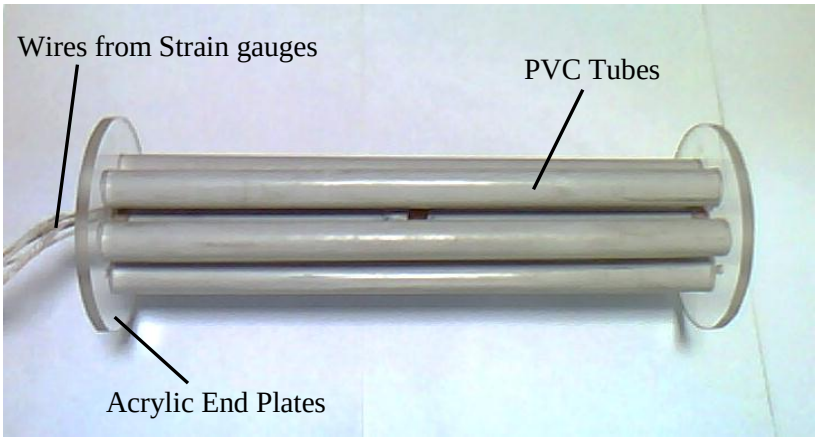

Figure 3.2: PVC tube bundle

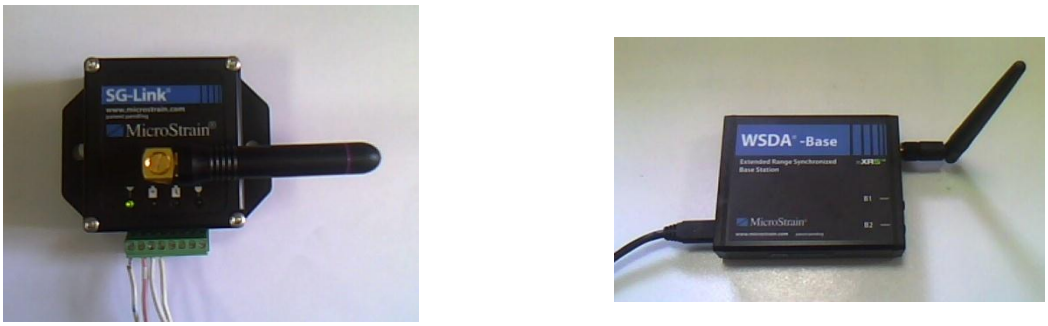

(a) **(b)**

Figure 3.3: (a) SG-Link wireless sensing node (b) WSDA USB base station

The figure 3.4 presents the complete layout of the experiment.

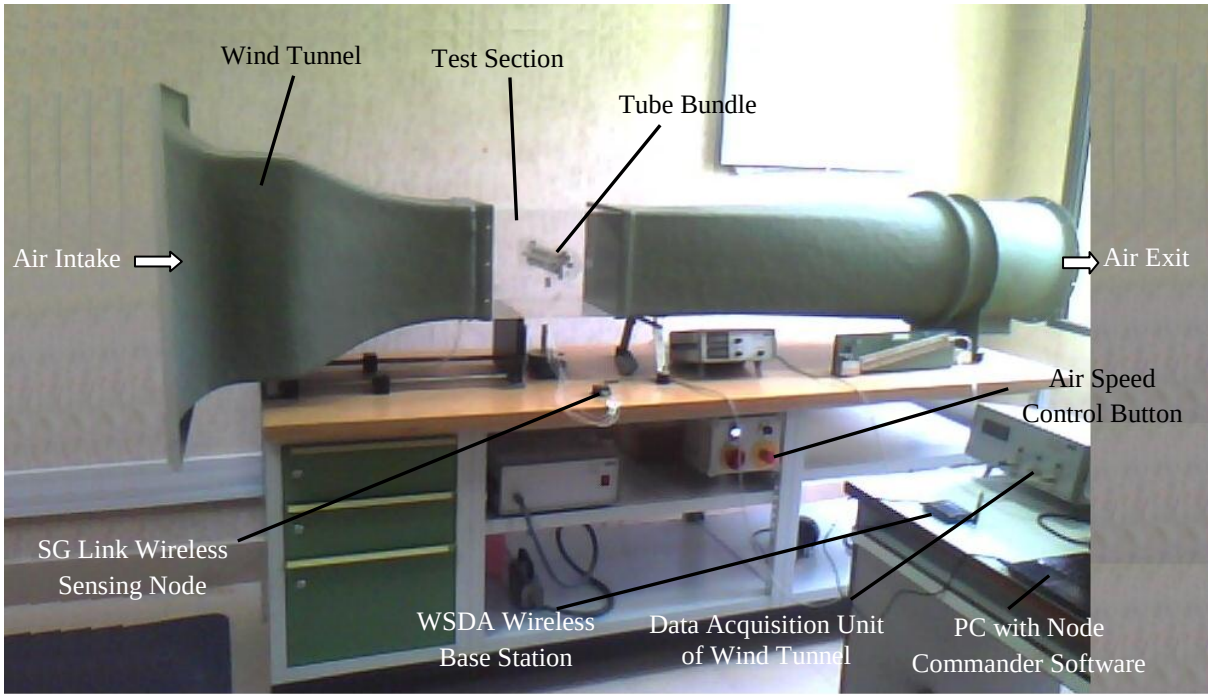

Figure 3.4: Experimental setup layout

3.3 Data Acquisition System

The vibration response is taken from the target tube by installing four strain gauges in full Wheatstone bridge circuit. This approach has been used by a number of researchers in recording flow-induced vibrations. Strain gauges from measurements group (EA-06-240LZ-120) are used for this purpose. The arrangement of strain gauges in full Wheatstone bridge circuit is presented in the figure 3.5.

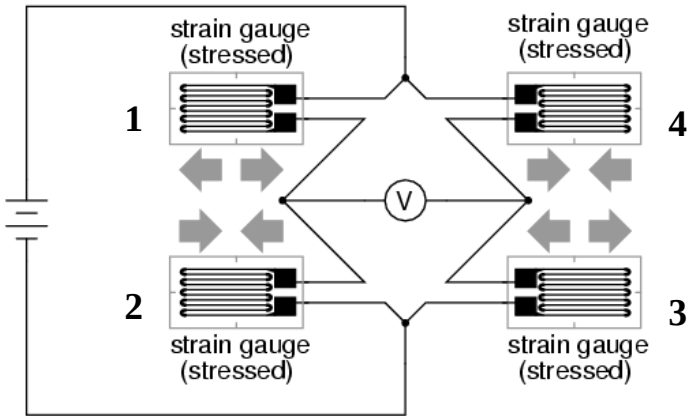

Figure 3.5: Full Wheatstone bridge strain gauge circuit

The strain gauges are attached on the tube in such a way that when gage 1 and 3 are in tension, the gage 2 and 4 are in compression and vice versa. The resulting strain produces a signal which is then sensed by SG-Link wireless sensing node and then covert that strain into displacement which is then used for the analysis.

The figure 3.6 presents the flow diagram of the data acquisition system.

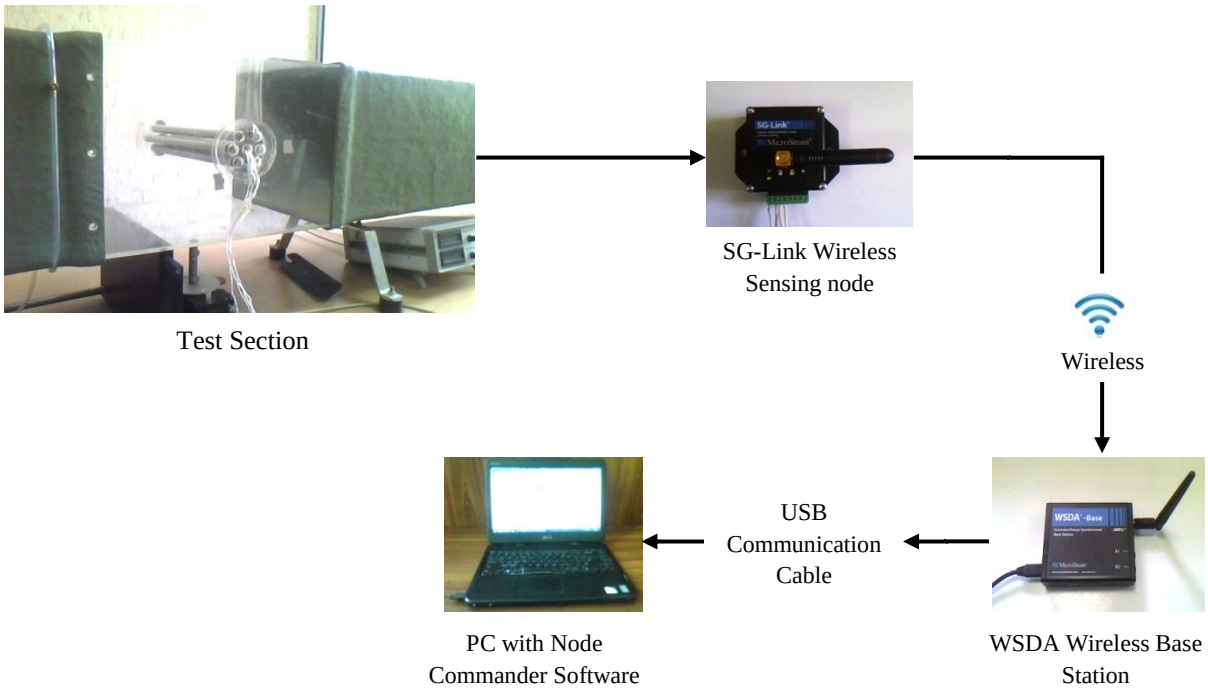

Figure 3.6: Data acquisition flow chart

3.3.1 Characteristics of Measuring Instruments

- **SG-link wireless sensing Node**: Used to capture data from the strain gages having accuracy of ± 0.1% of the full scale reading.
- **Maximum measuring range:** -5 mm to 5 mm
- **Data acquisition time:** 08 seconds
- **Sampling rate:** 736 samples / sec

3.4 Tube Bundle

In order to simulate heat exchanger tube bundle, a bundle of circular tubes made up of PVC is used. In practical heat exchangers, the tube arrays are arranged in a number of geometric patterns such as normal square, rotated square, normal triangular, rotated triangular and staggered. However, in current work the tube bundle is taken as rotated triangular bundle

(60˚) with a pitch of 24.9 mm as the criteria defined by Blevins (Blevins, 2001). Figure 3.8 shows drawing of the tube bundle with dimensions. Location of instrumented tube in the tube bundle is shown in figure 3.8. Table 3.1 presents the specifications of the tube bundle.

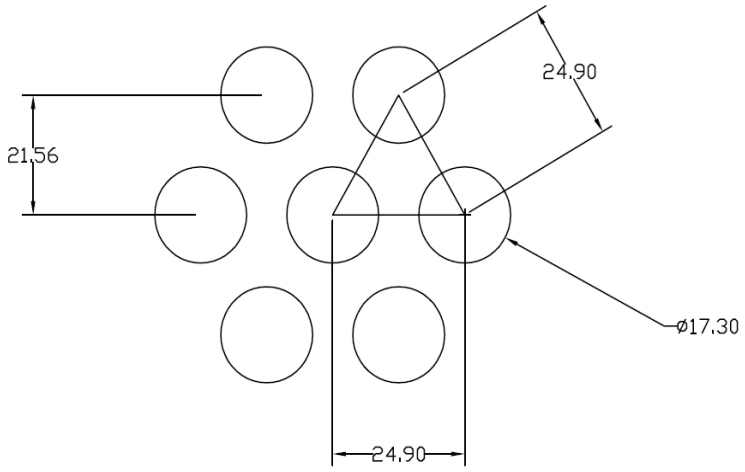

Figure 3.7: Tube bundle drawing (Dimensions are in millimeters)

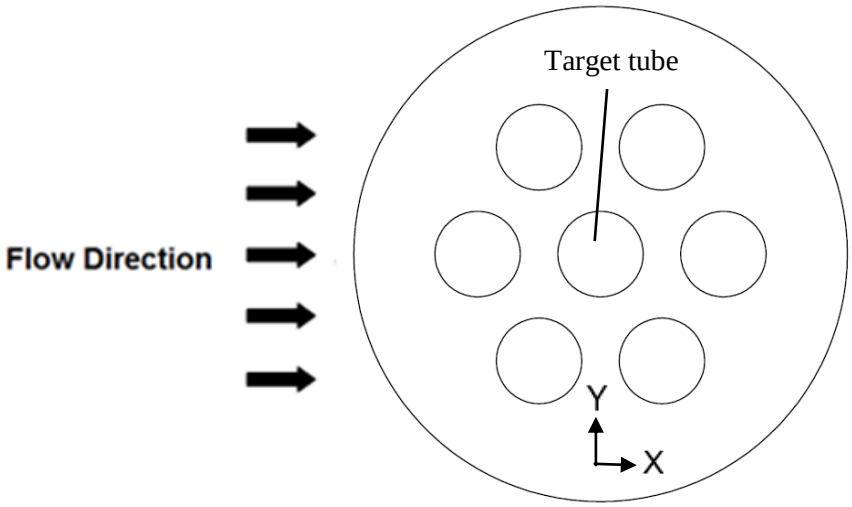

Figure 3.8: Location of Target tube in tube bundle

Table 3.1: Specifications of the tube bundle

Tube material	PVC
Number of tubes	7
Arrangement of tubes	Rotated triangular (60º)
Mass of tube	12 g
Tube outer/inner diameter	17.3 mm / 16.1 mm

End plate hole clearance	0.5 mm
Fluid / Temp.	Air / 24 ºC
Number of spans	1
Targeted span length	281 mm
Location of strain gauges	Mid-span
Pitch	24.9 mm
P/D ratio	1.44
Modulus of Elasticity (tube)	2 GPa (2.04×10^8 kg/m^2)
Density of tube	1400 kg/m^3
Density of air	1.2041 kg/m^3

3.5 Signal Analysis Software

The SIGVIEW software developed by SignalLab is used to analyze the signal taken from the sensors. It is powerful tool used to perform the spectral analysis. In this experimentation, this tool is used to perform Fast Fourier Transform (FFT) of the signal. The figure 3.10 presents the interface of the software.

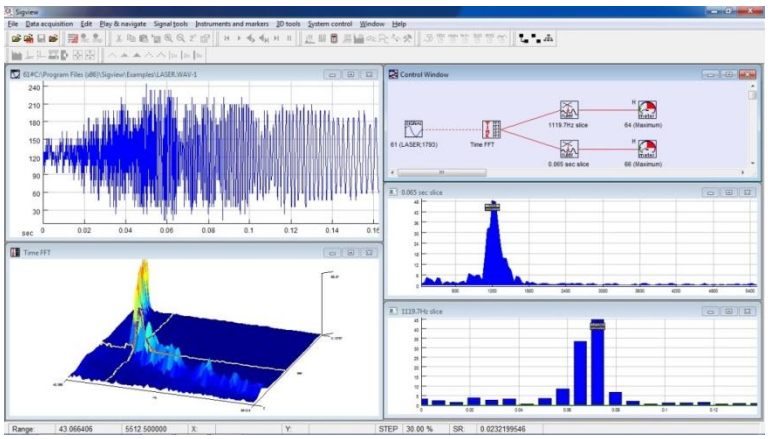

Figure 3.9: SIGVIEW software interface window

3.5.1 Features of SIGVIEW

The following are the features of the SIGVIEW software.

- It provides real time streaming with complete data display, signal analysis and control.
- Provides FFT transforms of the signal with multiple features.
- It also supports time-FFT and spectrograph features

- This software is specialized in signal filtering (lowpass, highpass etc.)
- It also performs real time arithmetic operations with all kinds of signals.
- Specialized in numerous statistical functions like averaging, probability distribution, averaging of the signals etc.
- User friendly interface and complete control window showing every operation performed on the signal.

3.6 Experimentation Conditions

The experimentation is carried out ($0.34 \times 10^4 \leq Re \leq 2.29 \times 10^4$) for a single target tube in the bundle as shown in the figure 3.9. The experimentation has two phases. In first phase, the target tube is set in such a way that the strain gauges record vibration amplitude in the flow direction at the mid-span of the tube. In the second phase, the target tube is rotated by 90^o to allow strain gauges to record the vibration amplitude in the lateral direction. For both phases, the span length is kept constant of length 281 mm. The free stream velocity is varied from 3 m/s to 20 m/s in the wind tunnel.

CHAPTER 4: EXPERIMENTAL RESULTS

4.1 Introduction

Experimentation has been carried out on a tube bundle made up of PVC tubes. The span has fixed boundaries and the middle tube in the bundle is instrumented with strain gages for measuring amplitude response; first in flow direction and then in the lateral direction. The following are the experimental results.

4.2 Experimental Results

4.2.1 Natural Frequency

Natural frequency is the lowest frequency at which a structure vibrates in the absence of any driving or damping force. In order to perform experimental analysis of the tube bundle, determination of natural frequency of the target tube is very important because it has a significant impact on tube vibration and can even cause tube failure and damage at the resonance conditions.

The following relation is used to determine natural frequency of the tube in a tube bundle with fixed boundaries (Blevins, 2001):

$$f_n = \frac{1}{2\pi}\left(\frac{\lambda_n}{l_s^2}\right)\sqrt{\frac{EI}{m}} \tag{4.1}$$

As tubes are made up of PVC, values for different properties of the target tube are as follows:

l_s = Tube span length = 0.281 m

E = Modulus of elasticity = $2 \times 10^9\ N/m^2$

I = Area moment of inertia = $\frac{\pi\,(d_o{}^4 - d_i{}^4)}{64}$ = $1.099 \times 10^{-9}\ m^4$

m = Mass of the tube per unit length = 0.0712 kg/m

λ_n = Frequency Constant = 22.4

From equation (4.1), f_n = 250.90 Hz

The FFT of vibration signal from the tube is found to be in good agreement with the analytically determined frequency as shown below in figure 4.1.

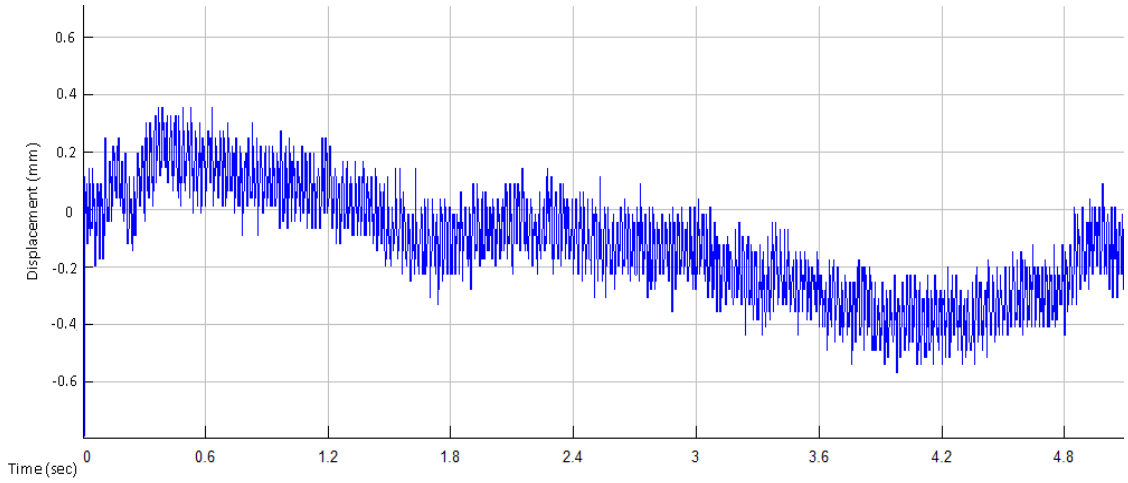

(a)

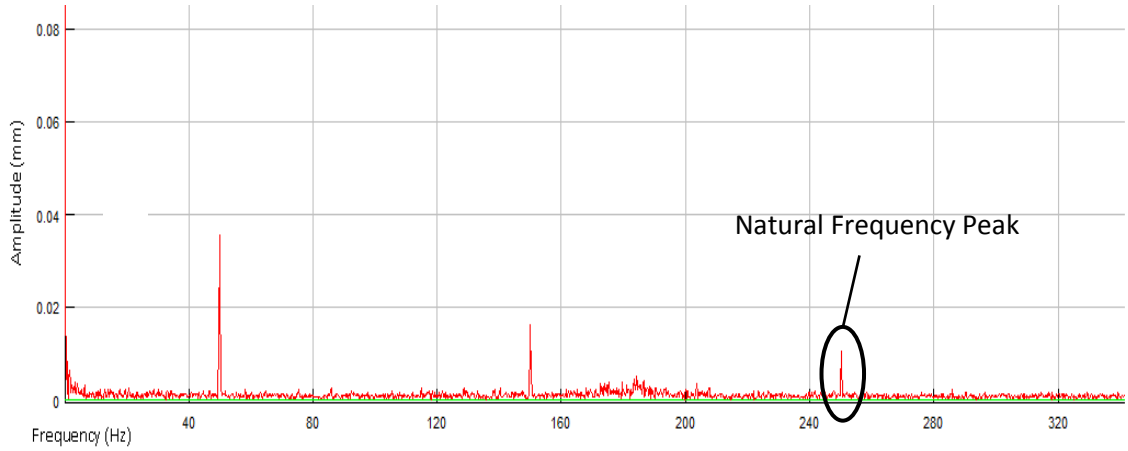

(b)

Figure 4.1: (a) Displacement-time signal of target tube (in flow direction) at $U_\infty = 3\ m/s$ (b) FFT plot of the signal

The FFT gives the value of natural frequency peaks ranging from 248 - 251 Hz and analytical method gives the value of 250.9 Hz, which are in good agreement with each other. The response (natural) frequency plots of the monitored tube under two orientation conditions are given in figure 4.2.

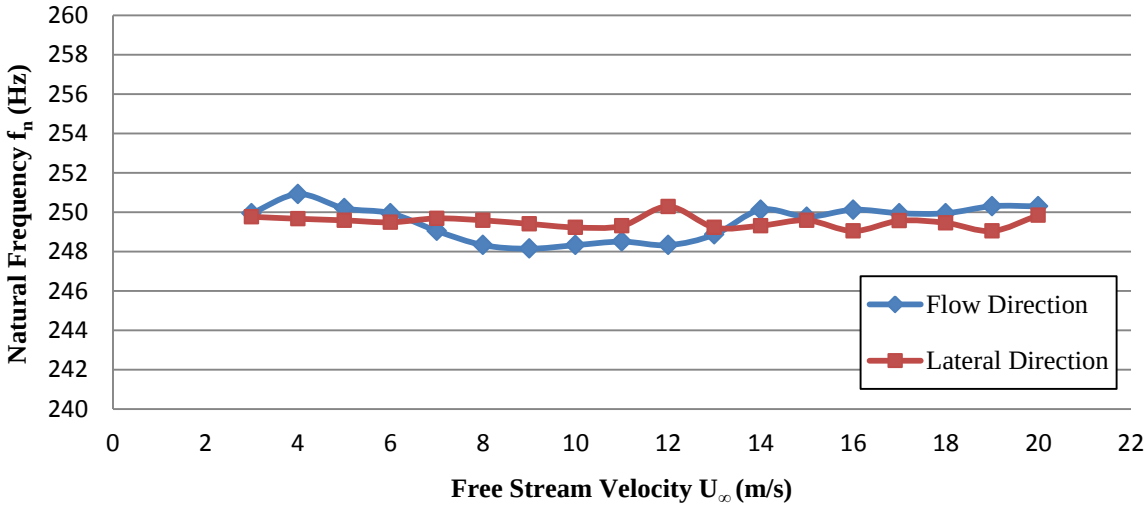

Figure 4.2: Natural (Response) frequency plot of target tube

4.2.2 Turbulent Buffeting Frequency

Turbulence in the shell side flow causes structural excitation to the tubes however it is helpful for better heat transfer. Turbulence in flow field is also caused by upstream rows of tubes in the tube bank. The low amplitude vibration in heat exchanger tubes caused by the turbulence in flow field is known as turbulent buffeting. Turbulent buffeting is characterized at a dominant frequency known as turbulent buffeting frequency. Turbulent buffeting frequency for gas flow normal to a tube bundle is given as (Owen 1975),

$$f_{tb} = \frac{U_\infty}{D X_L X_T}\left[3.05\left(1-\frac{1}{X_T}\right)^2 + 0.28\right] \tag{4.2}$$

Where X_L = longitudinal pitch ratio = P/D and X_T = transverse pitch ratio = T/D. In the low velocity range of 3 to 10 m/s, turbulent buffeting frequency comes out to be in the range of 39 to 128 Hz. In the current experiment, the FFT of displacement-time signal gives a peak in the range of 45 to 50 Hz at low free stream velocities of air which may be taken as turbulent buffeting frequency of the target tube as it is in good compliance with the analytical results. The figures 4.3 and 4.4 display the displacement-time plots and their FFTs. The black circle in each FFT plot indicates the turbulent buffeting frequency of the instrumented tube.

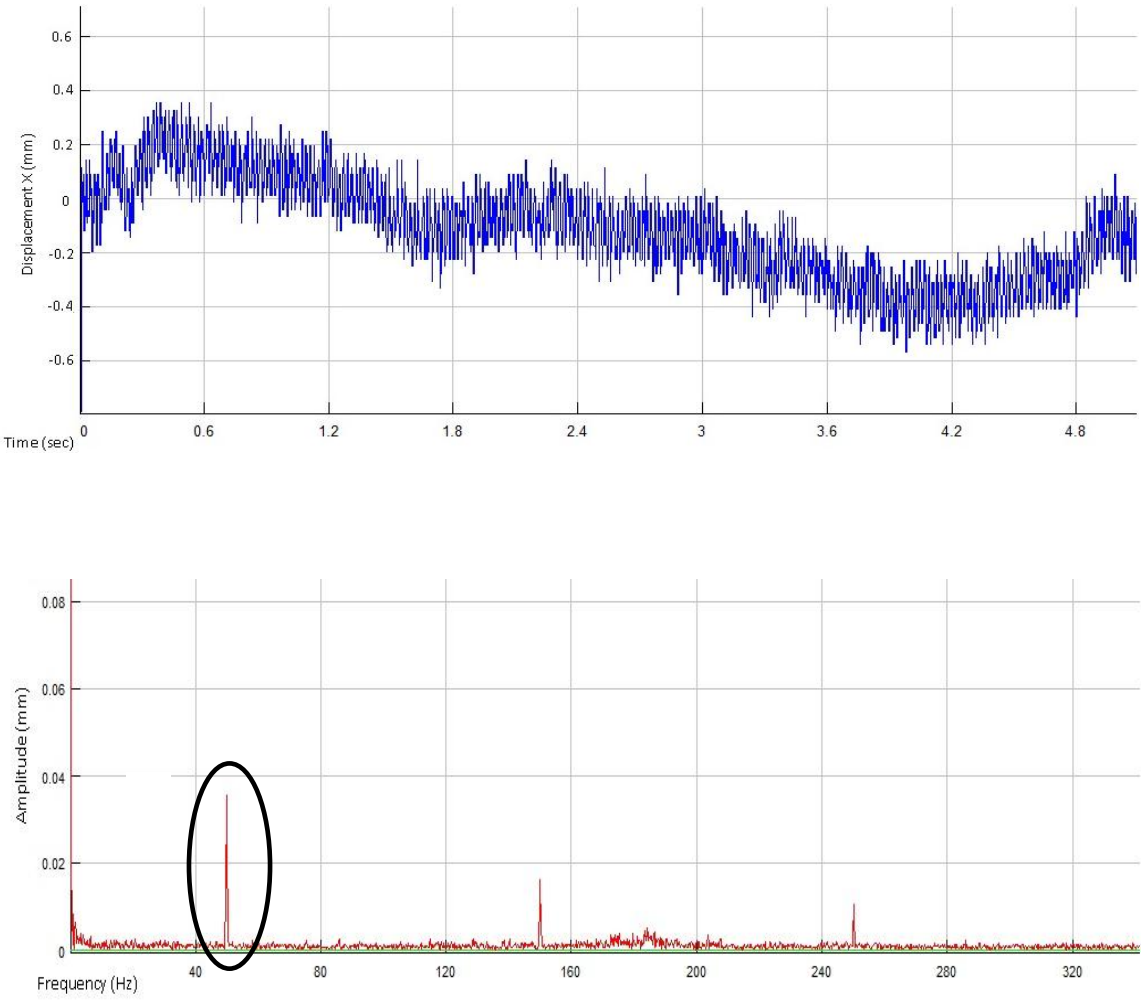

Figure 4.3: Target Tube Response (in flow direction) at $U_\infty = 3\ m/s$, $U_p = 9.83\ m/s$, $T = 24\ °C$

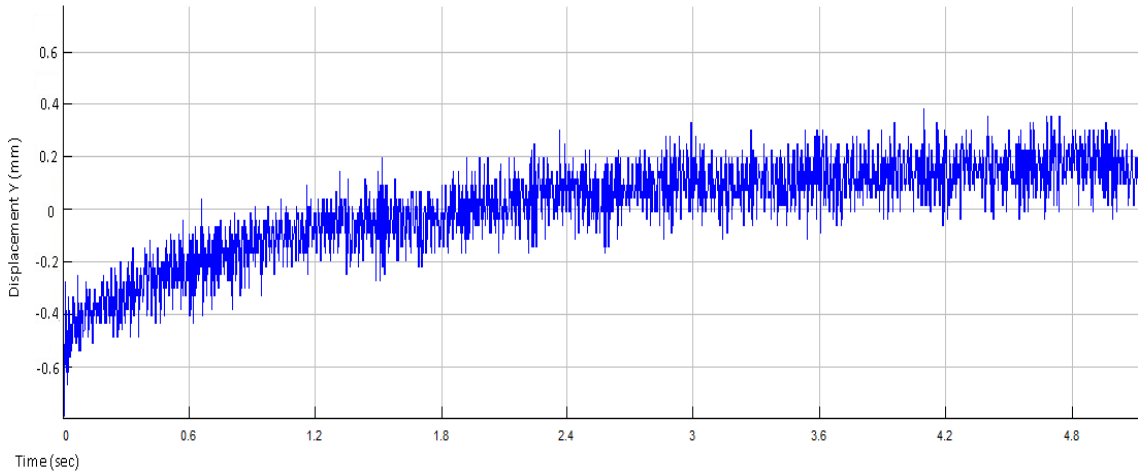

Figure 4.4 (a): Displacement Time Signal of Target Tube (in lateral direction) at $U_\infty = 3\ m/s$, $U_p = 9.83\ m/s$ and $T = 22\ °C$

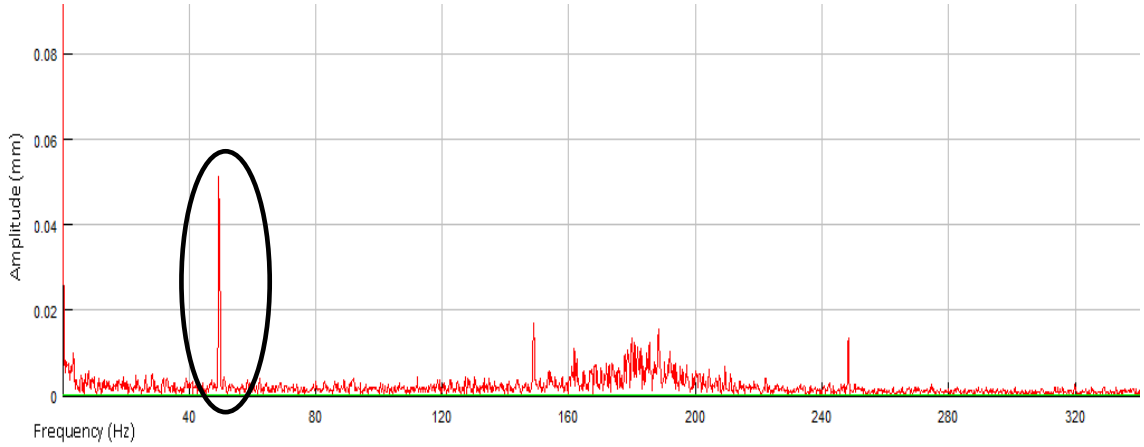

Figure 4.4 (b): Target Tube Response (in lateral direction) at $U_\infty = 3\ m/s$, $U_p = 9.83\ m/s$, $T = 22\ °C$

The plots of turbulent buffeting frequency against free stream velocity of the monitored tube under two orientation conditions are given in figure 4.5.

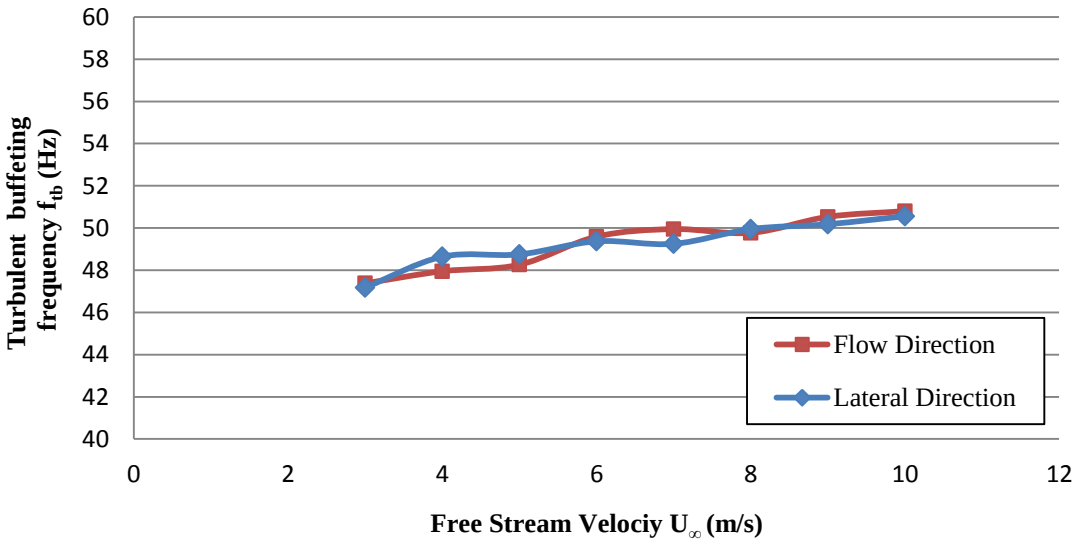

Figure 4.5: Turbulent buffeting frequency plot

As seen in the above figure, the turbulent buffeting frequency is consistent over the current range of velocity under two different conditions. This also concludes that the tubes are quite stable in this range of velocities, since the turbulent buffeting frequency is away from the natural frequency of tubes, so practically there is no chance of resonance.

4.2.3 Pitch Velocity and Reduced Velocity

For flow induced vibration analysis of tube bundles, the flow velocity is usually defined in terms of pitch velocity,

$$Pitch\ Velocity = \frac{U_\infty P}{P - D} \tag{4.3}$$

Where, U_∞ is the free stream velocity (i.e. the velocity that would exist if the tubes were removed), P is the pitch of tube bundle and D is the diameter of tubes. Another important parameter used in the vibration analysis of tube bundles is reduced velocity. The reduced velocity is computed by using following relation (Blevins, 2001).

$$Reduced\ Velocity = \frac{U}{f_n D} \tag{4.4}$$

Where U may be free stream velocity or pitch velocity, f_n is the tube's natural frequency and D is the tube diameter.

The table 4.1 presents the values of pitch velocity and reduced pitch velocity against free velocity for the current experiment.

Table 4.1: Pitch velocity and reduced pitch velocity of air flow

Sr. No.	Free stream velocity $U_\infty (m/s)$	Pitch / Gap velocity $U_p (m/s)$	Reduced pitch velocity U_r
1.	3	9.83	2.26
2.	4	13.11	3.02
3.	5	16.38	3.77
4.	6	19.66	4.53
5.	7	22.93	5.28
6.	8	26.21	6.04
7.	9	29.49	6.79
8.	10	32.76	7.55
9.	11	36.04	8.30
10.	12	39.32	9.06
11.	13	42.59	9.81
12.	14	45.87	10.57
13.	15	49.14	11.32

14.	16	52.42	12.08
15.	17	55.70	12.83
16.	18	58.97	13.59
17.	19	62.25	14.34
18.	20	65.53	15.10

4.2.4 Vortex Shedding

When fluid flows across a tube, vortices are generated at downstream of the tube and separate intermittently from either side of the tube. This periodic separation of vortices alternately from both sides of the tube in a cyclic manner result in fluctuating lift and drag forces which may cause periodic movement of the tube. This phenomenon occurs more repeatedly as the velocity of the flow increases and is known as vortex shedding. The vortex shedding frequency is given by the following relation (Blevins, 2001).

$$f_{vs} = \frac{St\ U_{\infty}}{D} \tag{4.5}$$

Strouhal number, St for current rotated triangular tube bundle with pitch to diameter ratio of 1.44 is estimated to be 0.25 (Fig. 3-5, p. 50, Blevins 2001). So the vortex shedding frequency for the test tube bundle can be calculated from the above relation. By analyzing FFT of the signal, a spectral peak is observed at nearly 150 Hz in addition to the peaks of turbulent buffeting frequency at 49 Hz and natural frequency at 250.9 Hz as shown in figure 4.6.

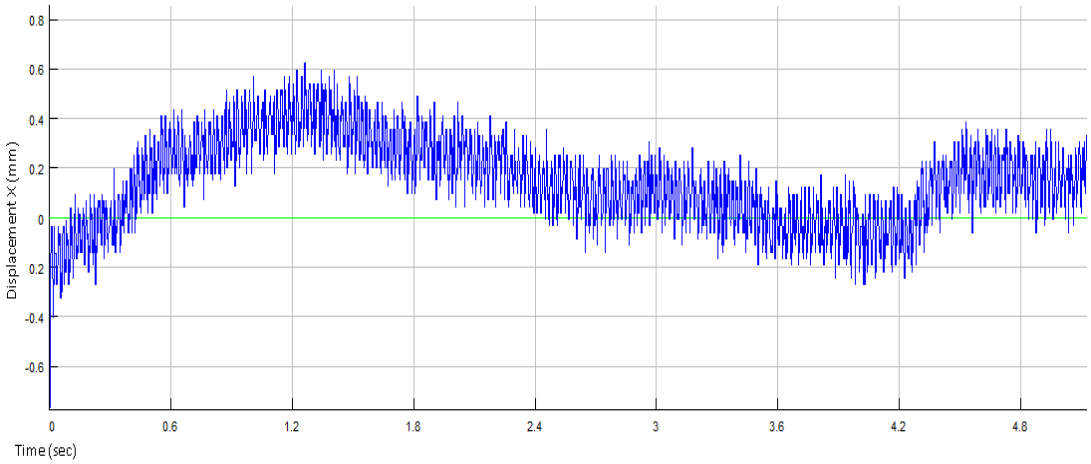

(a)

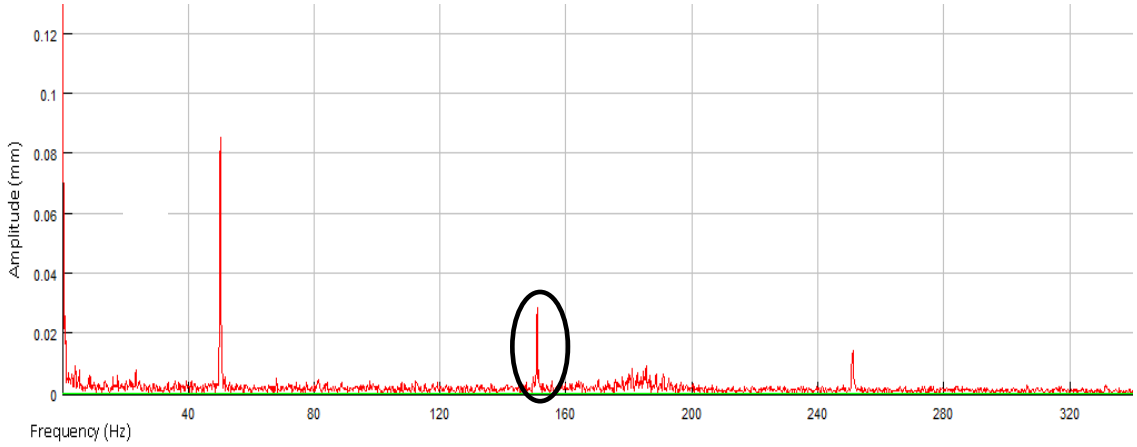

(b)

Figure 4.6: (a) Displacement time signal of target tube (b) FFT plot of target tube at $U_\infty = 5\ m/s$

This peak is thought to be the vortex shedding frequency. To confirm it, this frequency is plotted against free stream velocities presented in the figure 4.7.

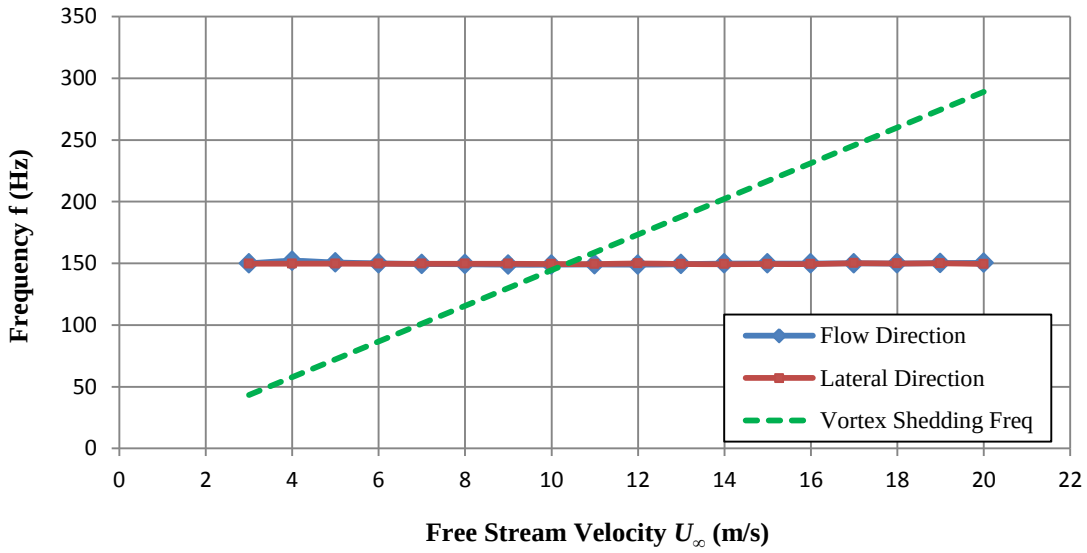

Figure 4.7: Observed frequency response

From the above plot, it is clear that the frequencies of the spectral peak remain constant over the current range of velocity. The plot indicates that this spectral peak should not be the vortex shedding frequency, because vortex shedding frequency varies directly with the flow velocity as shown in the plot as a dotted line.

The possible reason for this observed frequency is that it could be another natural frequency of the monitored tube. The monitored tube vibrating in flow may have more than one natural

frequency. These frequencies are due to impact of other tubes in the bundle which may force it to vibrate with more than one natural frequency.

4.2.5 Amplitude Response

The amplitude of vibration is represented as root mean square value of the output signal of strain gauges. Root mean square value can be used to compare the vibration amplitudes at different flow velocities. The rms amplitude is determined as

$$A_{rms} = \frac{1}{\sqrt{2}} A_{ins} \tag{4.6}$$

The vibration amplitude response acquired from the strain gauge sensors is given in appendix A. Table 4.2 presents the rms amplitude values of the instrumented tube in the tube bundle under two different orientation conditions (in flow and lateral directions).

Table 4.2: Amplitude response of target tube

Sr. No.	Free stream velocity $U_\infty (m/s)$	Reduced pitch velocity U_r	RMS Amplitude (mm)	
			In flow direction X_{rms}	In lateral direction Y_{rms}
1.	3	2.26	0.075	0.105
2.	4	3.02	0.086	0.058
3.	5	3.77	0.114	0.116
4.	6	4.53	0.084	0.131
5.	7	5.28	0.109	0.184
6.	8	6.04	0.143	0.158
7.	9	6.79	0.121	0.189
8.	10	7.55	0.149	0.222
9.	11	8.30	0.194	0.218
10.	12	9.06	0.164	0.271
11.	13	9.81	0.187	0.302
12.	14	10.57	0.249	0.345
13.	15	11.32	0.336	0.433
14.	16	12.08	0.489	0.583
15.	17	12.83	0.585	0.635
16.	18	13.59	0.665	0.787
17.	19	14.34	0.798	1.006
18.	20	15.10	0.981	1.149

The graphical plots for amplitude response of the monitored tube under two orientation conditions are given in figure 4.8.

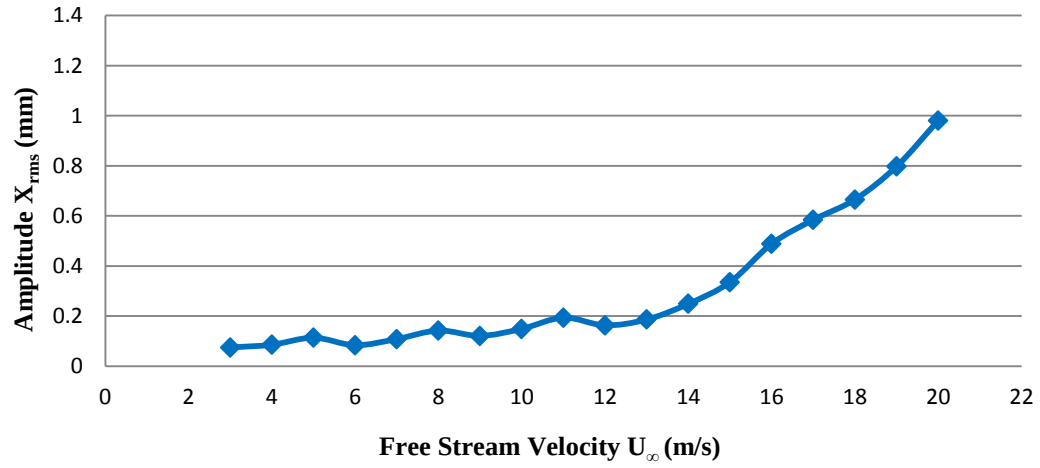

(a)

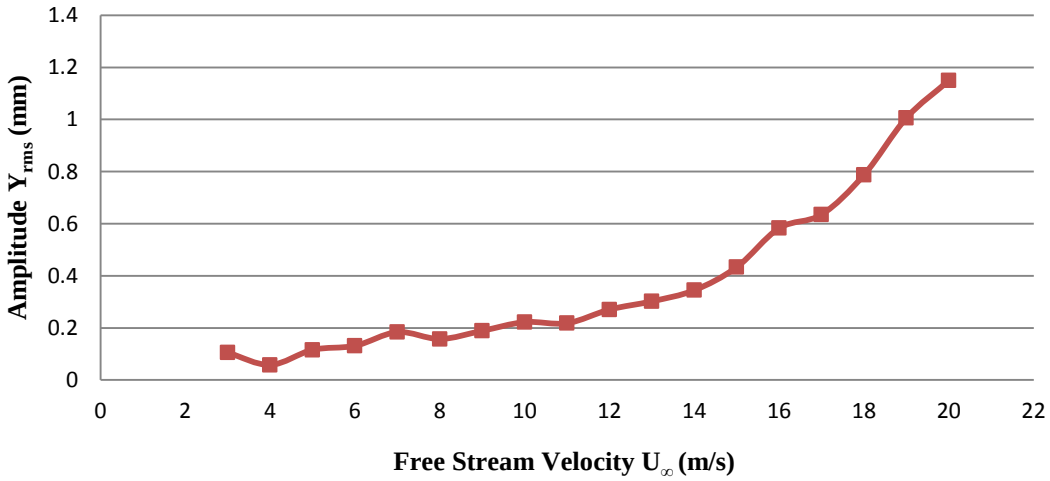

(b)

Figure 4.8: Vibration amplitude response (a) In flow direction (b) In lateral direction

The combined plot of rms amplitude response in the flow (X) and lateral (Y) directions is presented in the figure 4.9.

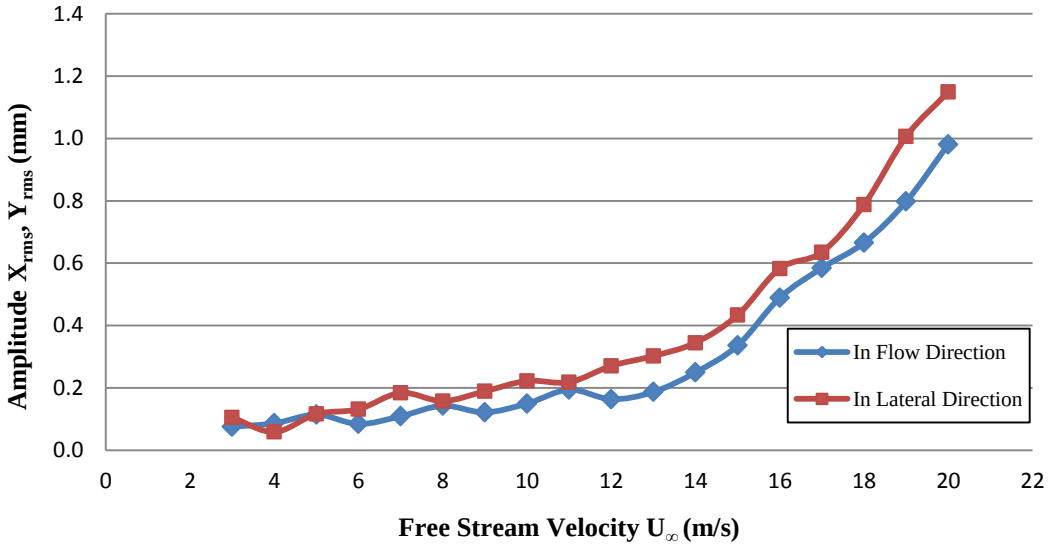

Figure 4.9: Vibration amplitude response of target tube

As seen in the figure 4.9, the two amplitude curves have a similar pattern with the increase in flow velocity. Initially vibration amplitudes are small and increase slightly with the flow velocity, when the velocity is below a critical value $U_\infty = 14\, m/s$. However, vibration amplitudes increase considerably as the flow velocity is increased above the critical velocity. Amplitude in the lateral (Y) direction is observed to be larger than that of the flow (X) direction. The small amplitude vibrations in the low velocity range are due to turbulence, while the significant enhancement of vibration amplitude with flow velocity indicates the occurrence of fluid elastic instability.

As fluid elastic instability is a self excitation phenomena, so the amplitude of vibration will continue to grow with increasing flow velocity as the critical instability velocity is surpassed. At and above critical flow velocity, a feedback mechanism exists between the vibrating tubes and the surrounding fluid so energy from the fluid flow is continuously transmitted to the tubes. As a result, the amplitude of vibration increases exponentially to unacceptable levels.

The combined plots of rms amplitude response in the flow (X) and lateral (Y) directions with pitch velocity and reduced pitch velocity are presented in the figures 4.10 and 4.11.

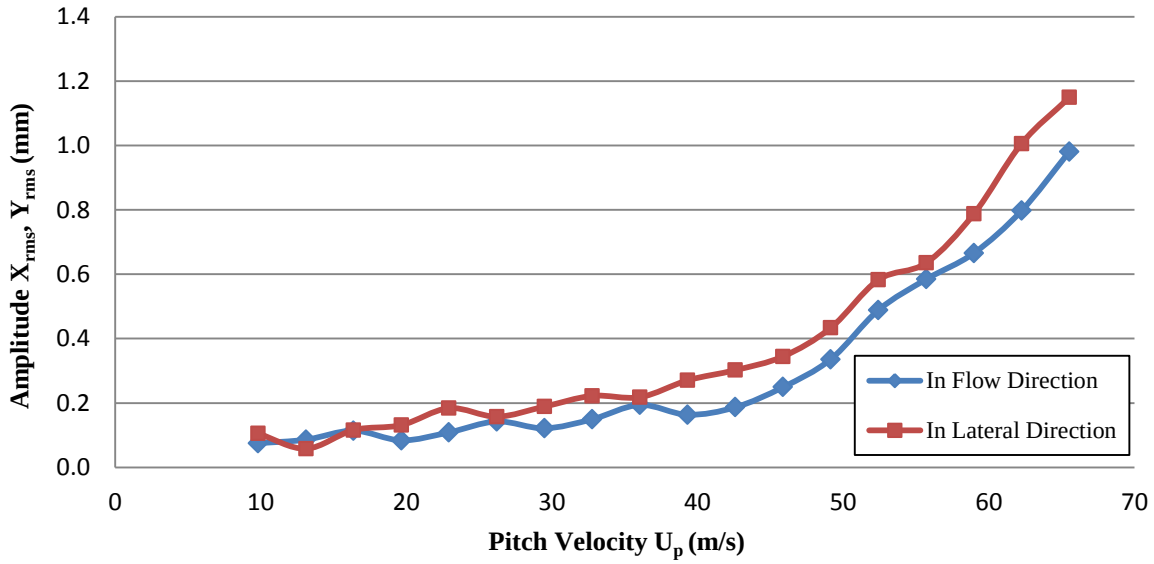

Figure 4.10: Vibration amplitude response of target tube with pitch velocity

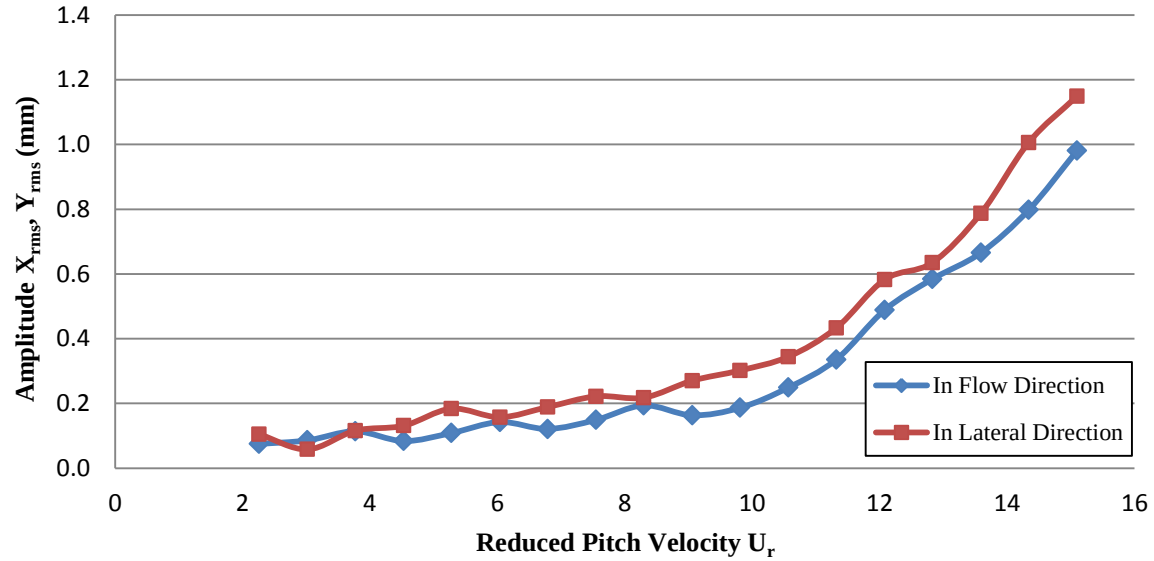

Figure 4.11: Vibration amplitude response of target tube with reduced pitch velocity

The combined plot of reduced amplitude response in the flow (X) and lateral (Y) directions as percentage of tube diameter is presented in the figure 4.12.

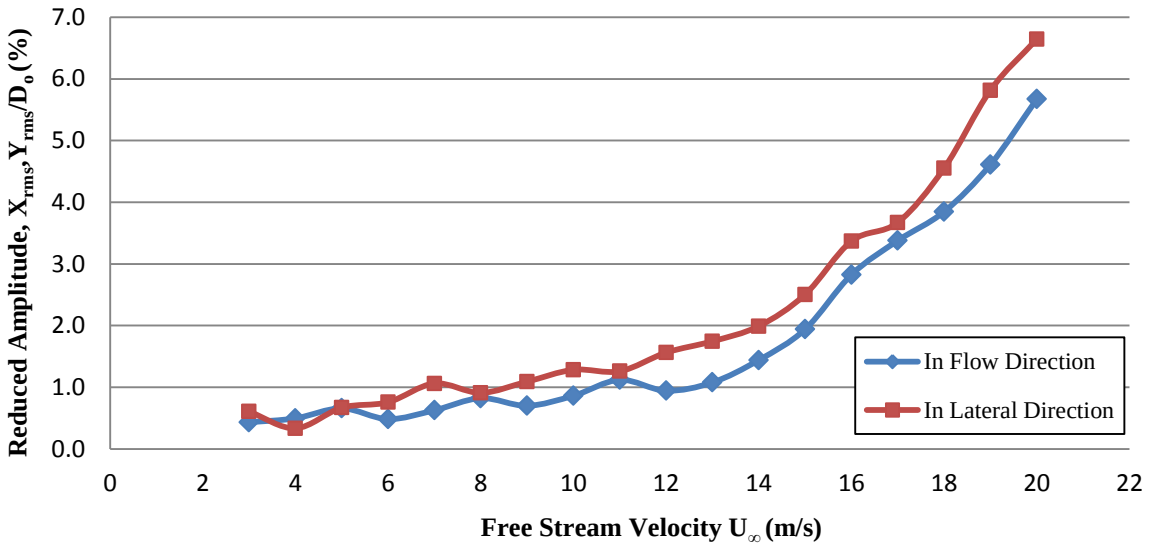

Figure 4.12: Reduced amplitude response of target tube

4.2.6 Hydrodynamic Mass

Hydrodynamics mass is defined as an effect which increases the apparent mass of the vibrating body due to the displacement of shell side fluid. The hydrodynamic mass has a significant impact on the amplitude of vibration. The hydrodynamic or added mass can be calculated for the triangular bundle using the following relation (Rogers et al., 1984).

$$m_h = \frac{\pi}{4}\rho_a {d_o}^2 \left[\frac{(d_{oe}/d_o)^2 + 1}{(d_{oe}/d_o)^2 - 1}\right] \tag{4.7}$$

Where d_{oe} is

$$\frac{d_{oe}}{d_o} = \left[0.96 + 0.5\left(\frac{P}{D}\right)\right]\left(\frac{P}{D}\right) \tag{4.8}$$

The total mass per unit length of the vibrating tube can be calculated as

$$m_t = m_{tube} + m_h + m_i \tag{4.9}$$

The total mass of the vibrating tubes is equal to the sum of original mass of the tube, mass of air disturbed by the tube during vibration and mass of the fluid flowing through the tube. In the current experiment, calculations of the total mass of tube are given as follows.

Original mass of tube = 12 g

Total length of tube = l_s = 281 mm

Original mass of the tube per unit length	=	m_{tube}	=	0.0427 g/mm
Hydrodynamic mass	=	m_h	=	0.0004 g/mm
Mass of the fluid inside tube	=	m_i	=	0 g/mm
Total mass per unit length	=	m_t	=	0.0431 g/mm = 0.0431 kg/m

4.2.7 Damping

Damping is any mechanism through which energy is dissipated during vibration. In fluid flow, oscillating structures are subjected to several forms of damping which operate at the same time. Damping has a strong impact on the amplitude of the vibration. Damping extracts energy from the vibrating body, thereby decreasing the amplitude of vibration. Therefore it plays an important role in flow induced vibrations of heat exchangers tube arrays. If the energy input to vibrating tubes cannot be dissipated in damping, the amplitude of the vibration increases dramatically leading to the structure failure. Damping ratio is estimated using the half-power bandwidth method (Bode's plot) which is based on the Fourier transform of the time domain amplitude signal of strain gauges as shown in figure 4.13 (Mitra, 2005).

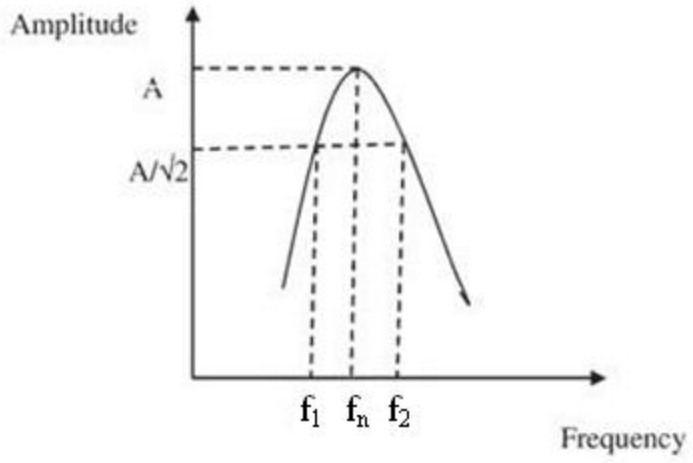

Figure 4.13: Bode's plot for damping (Mitra, 2005)

By using this plot and the analytical formula, the logarithmic decrement can be estimated as.

$$\zeta = \frac{f_2 - f_1}{2f_n} \tag{4.10}$$

$$\delta = 2\pi\zeta \tag{4.11}$$

The values of logarithmic decrement for the current experiment ranges from 0.003 to 0.009. The table 4.3 presents the values of logarithmic decrement against different flow velocities.

Table 4.3: Values of logarithmic decrement for target tube

Sr. No.	Free stream velocity $U_\infty (m/s)$	Pitch / Gap velocity $U_p (m/s)$	Reduced pitch velocity U_r	Logarithmic decrement δ	
				Flow Direction	Lateral Direction
1.	3	9.83	2.26	0.005153	0.005283
2.	4	13.11	3.02	0.008992	0.003774
3.	5	16.38	3.77	0.003628	0.005788
4.	6	19.66	4.53	0.005403	0.004533
5.	7	22.93	5.28	0.005550	0.005541
6.	8	26.21	6.04	0.004301	0.006044
7.	9	29.49	6.79	0.003290	0.004535
8.	10	32.76	7.55	0.004556	0.004536
9.	11	36.04	8.30	0.005057	0.005294
10.	12	39.32	9.06	0.003795	0.004284
11.	13	42.59	9.81	0.005556	0.004790
12.	14	45.87	10.57	0.005040	0.007812
13.	15	49.14	11.32	0.005285	0.006042
14.	16	52.42	12.08	0.004523	0.006782
15.	17	55.70	12.83	0.004525	0.008578
16.	18	58.97	13.59	0.004273	0.006797
17.	19	62.25	14.34	0.004266	0.006055
18.	20	65.53	15.10	0.004766	0.006543

The logarithmic decrement tells us about the level of damping in the tubes. It illustrates how fast the amplitude of vibrations is decaying with time. Logarithmic decrement plots in the flow (X) and lateral (Y) directions are presented in figure 4.14.

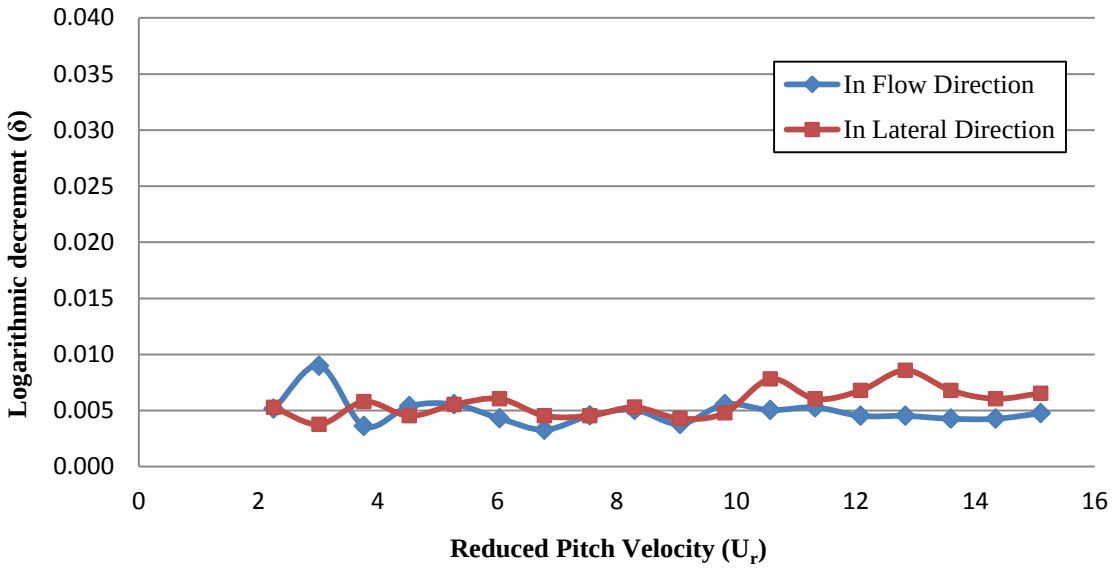

Figure 4.14: Damping plot of target tube

As seen in the graph, the value of logarithmic decrement almost remains constant over current range of velocities. The logarithmic decrement directly relates with damping. Higher the value of logarithmic decrement, higher the value of damping in the vibrating tubes.

4.2.8 Mass Damping Parameter

An important parameter called mass damping, reduced damping or Scruton number is used to estimate damping in vibrating structures and is given as:

$$Mass\ damping = \frac{m(2\pi\zeta)}{\rho D^2} \tag{4.12}$$

The mass-damping is very useful parameter to analyze the stability of a tube bundle subjected to flow induced vibrations. Vibrating mass of the structure has a strong influence on the damping of the structure. The table 4.4 presents the mass damping parameter values for instrumented tube for both orientation conditions.

Table 4.4: Mass damping parameter values

Sr. No.	Free stream velocity U_∞ (m/s)	Pitch / Gap velocity U_p (m/s)	Reduced pitch velocity U_r	Mass Damping Parameter ($m\delta/\rho D^2$)	
				Flow Direction	Lateral Direction
1.	3	9.83	2.26	1.0665	1.0773
2.	4	13.11	3.02	0.8687	0.9854

3.	5	16.38	3.77	0.7302	0.8045
4.	6	19.66	4.53	0.6583	0.7761
5.	7	22.93	5.28	0.6268	0.7166
6.	8	26.21	6.04	0.6112	0.7182
7.	9	29.49	6.79	0.5978	0.7169
8.	10	32.76	7.55	0.5998	0.6865
9.	11	36.04	8.30	0.5653	0.6279
10.	12	39.32	9.06	0.5404	0.6266
11.	13	42.59	9.81	0.5365	0.6572
12.	14	45.87	10.57	0.5367	0.5681
13.	15	49.14	11.32	0.5069	0.5379
14.	16	52.42	12.08	0.5060	0.5381
15.	17	55.70	12.83	0.5102	0.5377
16.	18	58.97	13.59	0.4502	0.5081
17.	19	62.25	14.34	0.4303	0.4477
18.	20	65.53	15.10	0.3903	0.4185

4.2.9 Stability Map

From the amplitude response of the monitored tube, it is clearly evident that there is a sharp change in the slope of tube vibration amplitude curve when the flow velocity is increased beyond a threshold velocity. This threshold velocity is known as critical velocity which is nearly 14 m/s in the current experiment. This indicates that fluid elastic instability has occurred in the tube bundle. In general, the stability of a tube bundle is expressed on a graphical plot known as the Connors' stability map in which mass damping parameter is plotted against the reduced velocity. Figure 4.15 presents the stability map for the current experimental data.

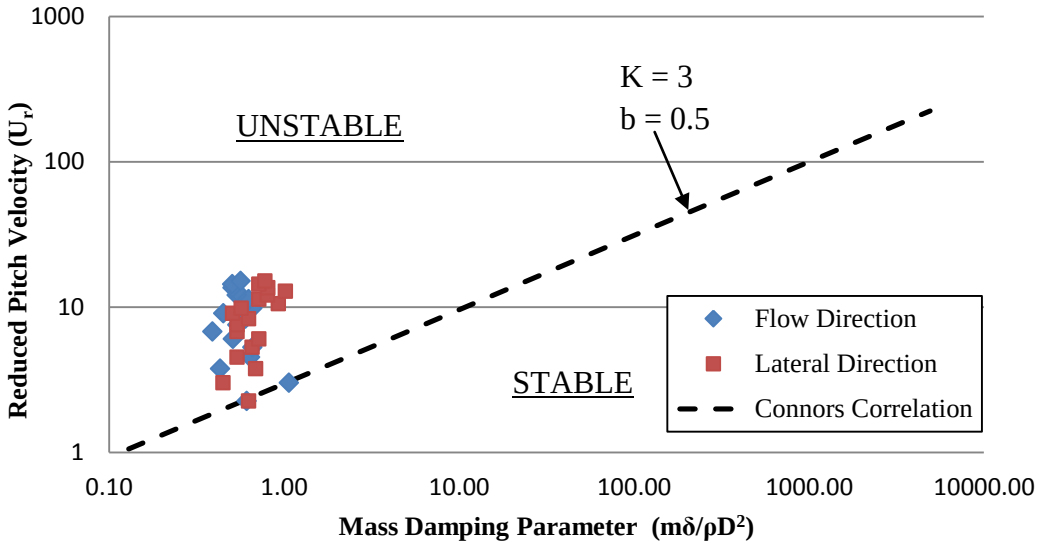

Figure 4.15: Mass-damping parameter vs reduced velocity (stability map)

The values of reduced pitch velocity obtained from Connors' correlation (with $K = 3$ and $b = 0.5$) for the present values of mass damping parameter are shown as dotted line. The plot indicates that the over the range of reduced pitch velocity from 2 to 15, mass damping parameter has very low values (less than 1), due to which the data points lie in the unstable region. This indicates that tube bundle is unstable in the current range of velocities and fluid elastic instability is inevitable.

4.2.10 Fluid Forces

When fluid flow over the tubes, it exerts force on the tube. These forces cause the tube to vibrate in all directions. The understanding of fluid forces is important in understanding the vibration behavior of tubes.

The following relation is normally used to estimate the drag forces acting on the tubes (Blevins, 2001).

$$F_D = \frac{1}{2}\,\rho {U_p}^2 d_o C_D \tag{4.13}$$

And the side forces can be estimated by using the following relation.

$$F_s = \frac{1}{2}\,\rho {U_p}^2 d_o C_s \tag{4.14}$$

The drag and side force coefficient can be calculated by analytical formulas used by many researchers (Roberts, 1966 and Connors, 1970).

$$C_D = 1 - \frac{d_o}{P} + \left(\frac{d_o}{P}\right)^2 \tag{4.15}$$

$$C_S = \left(\frac{d_o}{P}\right)^2 \tag{4.16}$$

In the present experiment, *P=24.9* mm, d_o*=17.3 mm*, the value of coefficients calculated by using equations 4.11 and 4.12 are

$C_D = 0.7879$ and $C_S = 0.4827$

By using the above values of force coefficients, the forces on the tube can be calculated by using equations 4.9 and 4.10. The table 4.5 presents the values of fluid forces per unit length on the target tubes.

Table 4.5: Fluid forces on the target tube

Sr. No.	Free stream velocity U_∞(m/s)	Pitch / Gap velocity U_p(m/s)	Fluid Forces	
			Drag Force (N/m)	Side Force (N/m)
1.	3	9.83	0.793	0.486
2.	4	13.11	1.411	0.865
3.	5	16.38	2.203	1.350
4.	6	19.66	3.173	1.944
5.	7	22.93	4.317	2.645
6.	8	26.21	5.640	3.455
7.	9	29.49	7.140	4.374
8.	10	32.76	8.811	5.398
9.	11	36.04	10.664	6.533
10.	12	39.32	12.693	7.777
11.	13	42.59	14.892	9.124
12.	14	45.87	17.274	10.583
13.	15	49.14	19.825	12.146
14.	16	52.42	22.560	13.822

15.	17	55.70	25.471	15.606
16.	18	58.97	28.550	17.492
17.	19	62.25	31.814	19.492
18.	20	65.53	35.255	21.600

The figure 4.16 presents the plots of the fluid forces against the pitch velocity.

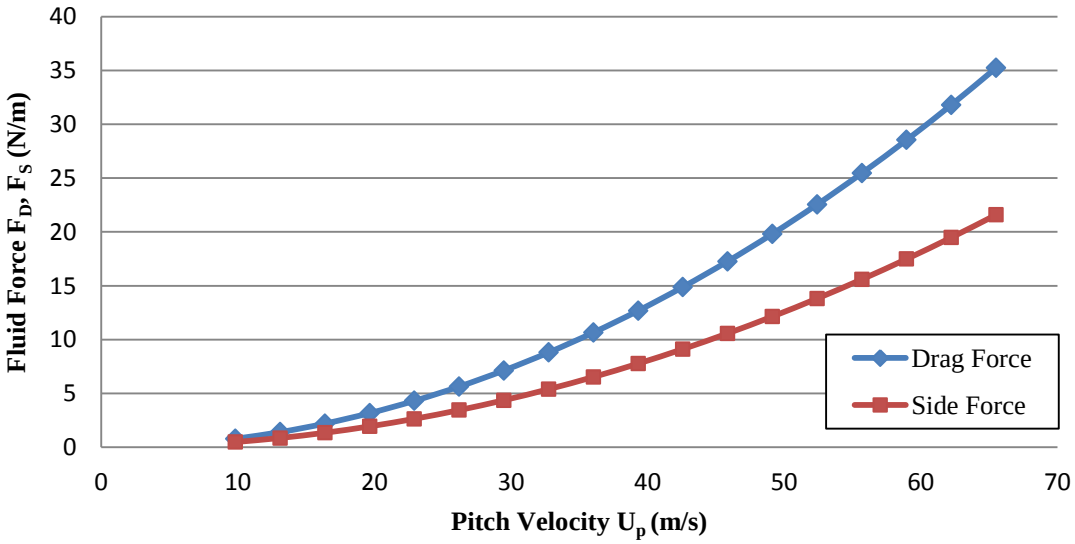

Figure 4.16: Fluid forces plot

As seen in the figure 4.16, the fluid forces vary directly with the velocity of the fluid. These fluid forces are of great concern in vibration analysis of the tube bundle. Generally, at high fluid velocities, there exists a phase difference between the displacements of the tubes and the fluid forces. This phase difference results in unbalance fluid forces on the tubes causing the tubes to become unstable. This instability is characterized as fluid elastic instability.

The figure 4.16 suggests that fluid forces generally increases with increase in the flow velocity. Higher the velocity, higher will be the fluid forces on the tubes and higher is the chance for tubes to become unstable.

4.3 Summary of Results

The measurement methodology is summarized in Table 4.6 and provides salient features of each measurement procedure. The summary of experimental results is given in appendix ‘B’.

Table 4.6: Summary of experimental methods for calculating flow induced vibration parameters

Parameter	Experimental Method
Frequency of vibration	FFT of Amplitude spectrum of strain-gauge signal
Amplitude	Rms value of strain gauge signal
Damping ratio	Frequency spectrum using bandwidth method (Bode's plot)
Flow velocity	Inclined-tube manometer of wind tunnel
Tube mass	Mass of tube in air + hydrodynamic mass
Fluid forces	Tube bundle geometry, density and velocity of inlet air
Temperature	Measured using thermometer

4.4 Results Comparison with the Past Research

The results comparison with the already published data gives a good way of validation of experimental data. There may be slight difference in the data due to difference in experimentation environment, material of tubes and other factors that affect the experimentation.

4.4.1 Comparison of Amplitude Response

The amplitude response is of central concern in vibration analysis of tube bundles because it gives information about the different vibration phenomena occurring inside the tube bundle due to the cross flow. The table 4.7 presents the comparison of experimental conditions of the current research work with the past experiments of Austermann et al. (1995) and Rottmann et al. (2003).

Table 4.7: Comparison of experimental conditions with past research

	Current Experiment	Austermann et al., 1995	Rottmann et al., 2003
P/D ratio	1.44	1.25	1.375
Tubes diameter (mm)	17.3	60	80
Arrangement of tubes	Rotated triangular (60˚)	Rotated triangular (60˚)	Rotated triangular (60˚)
Tube location	Central row	Central row	Central row
Tube material	PVC	Aluminium	Steel

Figure 4.17 presents the graphical comparison of the results of current experiment with the past experiments.

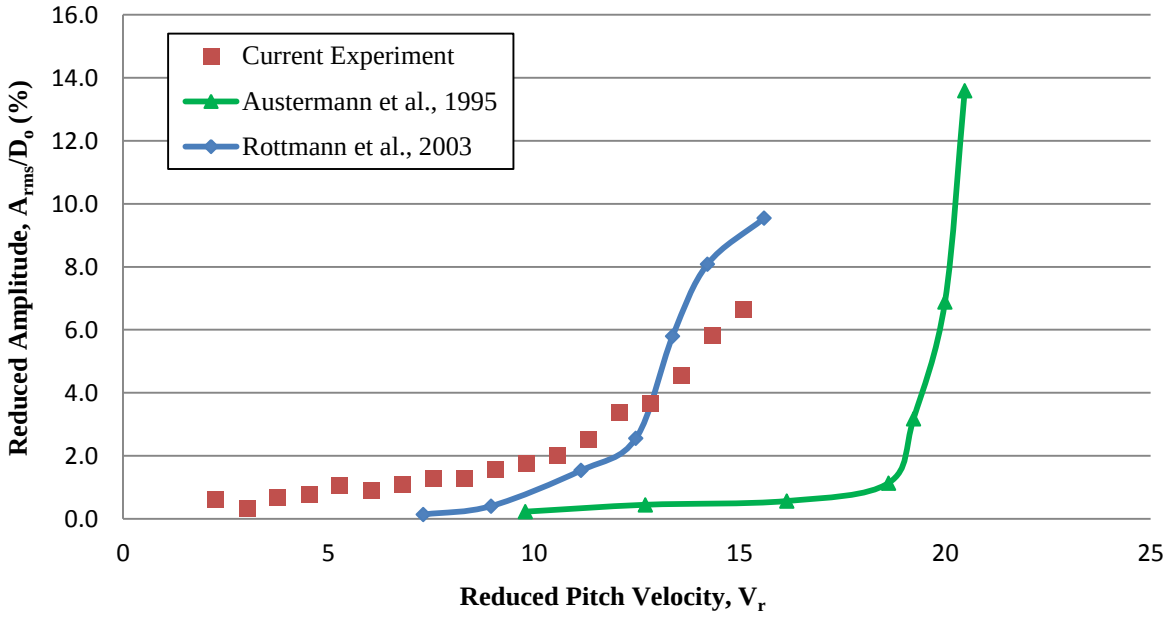

Figure 4.17: Amplitude response comparison of current experiment with past research

From the above plot of amplitude response, it is clear that there exists a good agreement of current experimental results with the past experiments. Because in the current experiment, tube bundle made up of PVC tubes is used, so the reduced amplitude is lower than that of the past researchers as they have used light metallic tubes for the tube bundles and higher cross flow velocities.

4.4.2 Comparison of Stability Behaviour

Stability behaviour of tube arrays is expressed by stability map in which the reduced pitch velocity ($U_r = U_p/f_n D$) is plotted as a function of the mass-damping parameter ($m\delta/\rho D^2$). The stability data for the current experiment is replotted in figure 4.18 together with comparable data from other researchers available in the open literature and the original stability boundary established for tube bundles by Connors (1978). His theoretical analysis suggested that the critical reduced velocity varies as the square root of mass damping parameter and his experiments proved good agreement with the theory for instability constant value, K = 3.0. Clearly, the results of the current study show a much smaller dependence of damping on the reduced pitch velocity.

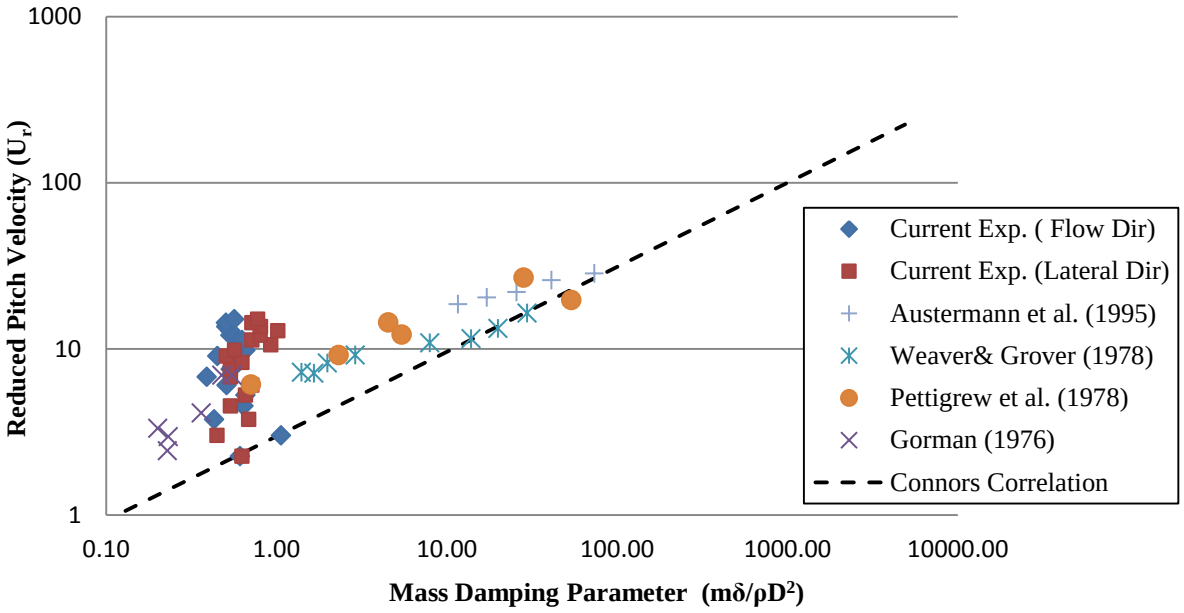

Figure 4.18: Comparison of stability behaviour of current experiment with published results for rotated triangular arrays (subjected to air cross flow)

The above plot shows that the data points from the present study lie within the scatter of the data reported by other researchers. However, most of the data points lie along the upper boundary suggesting a higher instability threshold for the current experiment.

CHAPTER 5: CONCLUSIONS AND RECOMMENDATIONS

Experimental investigations of cross flow induced vibrations in a tube bundle are carried out in this research work by conducting experiments in wind tunnel. Vibration behaviour of a single tube in a tube bundle has been examined by subjecting it to cross flow of air in a subsonic wind tunnel. The tube bundle consisted of seven PVC tubes with 17.3 mm outer diameter arranged in rotated triangular configuration. Tests are conducted in the wind tunnel over a range of free stream, air flow velocity from 3 to 20 m/s for which Reynolds number ranges from $0.34 \times 10^4 \leq Re \leq 2.29 \times 10^4$. The target tube is instrumented with strain gauges to measure the amplitude response in flow and lateral directions for each value of the upstream velocity. The displacement-time signal from strain gauges was collected using MicroStrain Inc. data acquisition system.

5.1 Conclusions

From the current experimentation and analysis, the following conclusions can be drawn.

- Amplitude of the monitored tube in the lateral (Y) direction is larger than that of the flow (X) direction due to rotated triangular (60^o) configuration of the tube bundle.
- Low amplitude vibrations of the monitored tube in low velocity range are due to turbulence in upstream flow, caused by the surrounding tubes.
- Vibration amplitudes increase significantly as the flow velocity is increased beyond a threshold velocity which indicates the onset of fluid elastic instability. The threshold velocity for fluid elastic instability to occur is known as critical velocity which is 14 m/s in the current experiment.
- Target tube vibrates with two distinct frequencies as presented in FFT of the vibration signal (figure 4.1). One of the frequencies is tube's own natural frequency and other frequency is due to the surrounding vibrating tubes.
- For flow velocity range of 3 m/s to 20 m/s used in the current experiment, vortex shedding phenomena is not observed.
- Low amplitude vibrations due to turbulent buffeting cannot be avoided in heat exchanger tube bundles, as considerable turbulence levels are always present. However, vibration level can be decreased appreciably by shortening the span length, decreasing the flow velocity and redistribution of flow.

- The damping response in both cases (flow and lateral directions) remains nearly same over the current velocity range.
- The stability map shows that tube bundle is unstable in the current range of velocities and fluid elastic instability is inevitable. The occurrence of fluid elastic instability can be avoided by either keeping the cross flow velocities below the critical velocity or by controlling the natural frequency and damping ratio of the tubes.

5.2 Recommendations for Future Work

The recommendations for the further work on the current experimental equipment are as follows.

- To investigate the amplitude response of the tubes (analyzed in the current experiment) under high ranges of Reynolds number.
- To investigate flow induced vibration phenomena using different tube bundle configurations in the wind tunnel.
- To explore the effect of P/D ratio, material of tubes and nature of fluid on flow induced vibrations of tube bundles in cross-flow.
- To investigate the three-dimensional lift, drag and axial response of the tubes under high ranges of Reynolds number.
- To place the monitored tubes at different locations in the bundle and investigate the lift, drag and axial response of the tubes. Also instrument the tube located at the exit of bundle and compare the vibration response of the tubes at three different locations in the tube bundle along a flow line.
- To investigate flow induced vibration phenomena using different tube bundle configurations in water tunnel .
- To investigate the effect of flow induced vibrations on heat transfer characteristics of tube bundles of shell and tube heat exchanger.

REFERENCES

- Austermann, R., and Popp, K., 1995, “Stability behaviour of a single flexible cylinder in rigid tube arrays of different geometry subjected to cross-flow”, Journal of Fluids and Structures, 9, 303–322.
- ASME Boiler and pressure vessel code (BPVC), Edition 2009.
- Blevins, R. D., 1974, “Fluidelastic whirling of a tube row”, ASME Journal of Pressure Vessel Technology, Vol. 96, pp. 263-267.
- Blevins, R. D., 1979, "Fluid damping and the whirling instability of tube arrays", In flow-Induced Vibrations (eds. S. S., Chen and M.D. Bernstein), New York; ASME, pp. 35-39.
- Blevins, R. D., 1984, "Review of sound induced by vortex shedding from cylinders", Journal of Sound and Vibration, 92, pp. 455-470.
- Blevins, R.D., 1990, “Flow-Induced Vibration”, Second ed., Van Nostrand Reinhold, New York.
- Blevins, R. D., 2001, “Flow-induced vibration”, Second edition, Krieger Publishing Company, Florida.
- Chen, Y. N. and Weber, M., 1970, "Flow induced vibrations in tube bundle heat exchangers with cross flow and parallel flow", Proceedings of ASME Symposium on Flow induced vibrations in heat exchangers, New York, pp. 57-77.
- Chen, S.S., Wambsganss, M.W., 1974, "Design guide for calculating natural frequencies of straight and curved beams on multiple supports", Components Technology Division, Argonne National Laboratory, Argonne, Illinois.
- Chen, Y. N., 1977, “The sensitive tube spacing region of the tube bank heat exchangers for fluid-elastic coupling in cross-flow”, Proceedings of ASME Symposium on Fluid-Structure Interaction Phenomena in Pressure Vessel and Piping Systems, pp. 1-18.
- Chiang, C.H., Liao, Y.C., Yu, M.H., 2005, “Flow induced vibrations of a triangular tube array in various arrangements of orientation and natural frequency”, Journal of the Chinese Institute of Engineers, 28, pp. 605-616.

- Chen, S.S., 1984, “Guidelines for the instability flow velocity of tube arrays in cross flow”, Journal of Sound and Vibration, 93(3), pp. 439-455.
- Chenoweth, J. M., 1993, Heat Exchanger Design Handbook, Hemisphere Publishing Corporation.
- Chung, H. J., & Chu, I. C., 2006, “Fluid-Elastic Instability of Rotated Square Tube Array in an Air-Water Two-Phase Cross-Flow”, Nuclear Engineering And Technology, Vol.38, No.1, 69-80.
- Connors, H. J., 1970, “Fluid-elastic vibration of tube arrays excited by the cross flow”, Flow Induced vibrations in Heat Exchangers, ASME, pp. 42-56.
- Connors, H.J., 1978, “Fluidelastic vibration of heat exchanger arrays”, ASME Journal of Mechanical Design, 100, pp. 347 – 353.
- Duro, V., Decultot, D., Leon, F., and Maze, G., 2011, “Experimental investigation on self-excited resonances of a cylindrical tube in cross-flow” Journal of Acoustical Society of America,129(5), pp. 184-189.
- Eisinger, F. L., Sullivan, R. E., 2007, “Acoustic resonance in a package boiler and its solutions - A case study”, Journal of Pressure Vessel Technology, 129, pp. 759 - 762.
- Elliott, G.L., and Pick, R.J., 1973, "Calculation of natural frequencies of heat exchanger tubes", Proceedings of International Symposium on Vibration Problems in Industry", Keswick, U.K.
- Endres, L. A. M., Moller, S. V., 2009, “Experimental study of the propagation of a far-field disturbance in the turbulent flow through square array tube banks”, Journal of the Braz. Soc. of Mech. Sci. & Eng., Vol. XXXI, No. 3, pp. 232-242.
- Fitzhugh, J. S., 1973, "Flow induced vibrations in heat exchangers", Proceedings of International Symposium on vibration problems in industry, U. K., Paper 427.
- Feenstra, P. A., Weaver, D. S., Eisinger, F. L., 2005, “Acoustic resonance in a staggered tube array: Tube response and the effect of baffles”, Journal of Fluids and Structures, 21, pp. 89–101.
- Gelbe, H., Jahr, M., Schroder, K., 1995, “Flow-induced vibrations in heat exchanger tube bundles”, Chemical Engineering and Processing, 34. pp. 289-298.
- Gorman, D.J., 1976, “Experimental development of design criteria to limit liquid cross-flow induced vibration in nuclear reactor heat exchange equipment”, Nuclear Science and Engineering, 61, pp. 324-336.

- Goyder, H.G.D., 2002, “Flow-induced vibrations in heat exchangers”, Trans IChemE, 80, pp. 226-232.
- Grover, L. K., Weaver, D. S., 1978, “Cross-flow induced vibrations in a tube bank – Vortex Shedding”, Journal of Sound and Vibration, 59(2), pp. 263-276.
- Hamakawa, H., Muraoka, K., Nishida, E., 2011, “Vortex shedding from tube banks with closely mounted serrated fin”, Journal of Environment and Engineering, 6, pp. 69-80.
- Hanson, R., Mohany, A., Ziada, S., 2009, “Flow-excited acoustic resonance of two side-by-side cylinders in cross flow,” Journal of Fluids and Structures, 25, pp. 80–94.
- Hassan, A. Marwan., Rogers, R. J., & Gerber, A. G., 2011, “Damping-Controlled fluidelastic instability forces in multi-span tubes with loose supports”, Nuclear Engineering and Design, 241, pp. 2666–2673.
- Hassan, M., & Hayder, M., 2008, “Modeling of fluidelastic vibrations of heat exchanger tubes with loose supports”, Nuclear Engineering and Design, 238, pp. 2507–2520.
- Hofmann, P. J., and Schettler, T., 1989, "PWR steam generator tube fretting and fatigue wear", EPRI report NP-6341.
- Inada, F., Kawamura, K., Yasuo, A., and Yoneda, K., 2002, “An experimental study on the fluid elastic forces acting on a square tube bundle in two-phase cross-flow” Journal of Fluids and Structures, 16, pp. 891–907.
- Iqbal, Q. and Khushnood, S., 2010, “Techniques for thermal damping in tube bundles”, Mehran University Research Journal of Engineering & Technology, 29 (4), pp. 635-646.
- Jones, A.T., 1970, "Vibration of beams immersed in liquid", Experimental Mechanics, pp. 84-88.
- Khalifa, A., Weaver, D. and Ziada, S., 2012, “A single flexible tube in a rigid array as a model for fluidelastic instability in tube bundles”, Journal of Fluids and Structures, 34, pp. 14–32.
- Khushnood, S., 2005, “Vibration analysis of a multi-span tube in a bundle”, Ph.D Thesis, Department of Mechanical Engineering, College of Electrical and Mechanical Engineering, National University of Science and Technology, Rawalpindi, Pakistan.
- Khushnood, S., Khan, Z. M., Koreshi, Z U., and Rashid, H. U., 2000, "Dimensional analysis of vibration of tube bundle in cross-flow", Proceedings of 2nd International

Symposium on Mechanical Vibrations, ISMV-2000, eds. Chohan G.Y., and Ameer M., Sept. 25-28, Islamabad, Pakistan, pp. 534-550.

- Khushnood, S., Khan, Z.M., Malik, M. A., Koreshi, Z., Javaid, M. A., Khan, M. A., Qureshi, H. A., Nizam, L. A., Bashir, K. S., Hussain. S. Z., 2012, "Cross-flow-induced-vibrations in heat exchanger tube bundles: A Review" book chapter in book titled "Nuclear Power Plants", Edited by Soon Heung Chang, ISBN 978-953-51-0408-7, InTech.
- Kissel, J. H., 1972, "Flow-Induced vibrations in Heat Exchangers-A practical look", 13th N. Heat Transfer Conference, Denver, AICh.E, paper 8.
- Lam, K., Lin, Y. F.,Zou, L., Liu, Y., 2010, "Experimental study and large eddy simulation of turbulent flow around tube bundles composed of wavy and circular cylinders", International Journal of Heat and Fluid Flow, 31, pp. 32–44.
- Liang, C., Papadakis, G., and Luo, X., 2009, "Effect of tube spacing on the vortex shedding characteristics of laminar flow past an inline tube array: A numerical study," Computers & Fluids, 38, pp. 950–964.
- Lowery, R.L., and Moretti, P.M., 1975, "Natural frequencies and damping of tubes on multi-span supports", 15th National Heat Transfer Conference, AIChE, Paper No.1, San Francisco.
- Mahon, J., and Meskell, C., 2009, "Investigation of the Underlying Cause of the Interaction between Acoustic Resonance and Fluidelastic Instability in Normal Triangular Tube Arrays", Journal of Sound and Vibration, 324, 91 – 106.
- Meskell, C., Fitzpatrick, J.A., 2003, "Investigation of the nonlinear behaviour of damping controlled fluidelastic instability in a normal triangular tube array", Journal of Fluids and Structures, 18, pp. 573 – 593.
- Mitra, D., Dhir, V. K., & Catton, I., 2009, "Fluid-elastic instability in tube arrays subjected to air-water and steam-water cross flow", Journal of Fluids and Structures, 25, pp. 1213 – 1235.
- Moretti, P. M., Lowery, R. L., 1976, "Hydrodynamic inertia coefficients for a tube surrounded by rigid tube", ASME Journal of Pressure Vessel Technology, 98, pp. 190–193.
- Mureithi, N. W., Zhang, C., Ruel, M., Pettigrew, M. J., 2005, "Fluidelastic instability tests on an array of tubes preferentially flexible in the flow direction", Journal of Fluids and Structures, 21, pp. 75–87.

- Lin, T.K., Yu, M.H., 2005, “An experimental study on the cross-flow vibration of a flexible cylinder in cylinder arrays”, Experimental Thermal and Fluid Science, 29, pp. 523-536.
- Oengoeren, A., Ziada, S., 1998, “An in-depth study of vortex shedding, acoustic resonance and turbulent forces in normal triangle tube arrays”, Journal of Fluids and Structures, 12, pp. 717 – 758.
- Ojalvo, I.U., and Newman, M., 1964, "Natural frequencies of clamped ring segments", Machine Design, pp. 219-222.
- Olinto, C. R., Augusto, L., Endres, M. and Moller, S. V., 2007, “Experimental study of the characteristics of the flow in the first rows of tube banks”, Transactions, SMiRT 19, Toronto.
- Owen. P.R., 1975, “Buffeting excitation of boiler tube vibration”, J. Mech. Eng. Sci., 4, pp. 431-439.
- Paidoussis, M. P., 1981, “Fluidelastic vibration of cylinder arrays in axial and cross flow: State of the art”, Journal of Sound and Vibration, 76, pp. 329-360.
- Paidoussis, M. P., 1982, “A review of flow-induced vibrations in reactors and reactor components”, Nuclear Engineering and Design, 74, pp. 31-60.
- Paidoussis, M. P., 2006, “Real-life experiences with flow-induced vibration”, Journal of Fluids and Structures, 22, pp. 741-755.
- Paul, S. S., Ormiston, S. J., Tachie, M. F., 2008, “Experimental and numerical investigation of turbulent cross-flow in a staggered tube bundle”, International Journal of Heat and Fluid Flow, 29, pp. 387–414.
- Paula, A. V., Endres, L. A. M., Moller, S. V., 2012, "Bistable features of the turbulent flow in tube banks of triangular arrangement", Nuclear Engineering and Design, 249, pp. 379–387.
- Payen, T., Villard, B., and Jalaldeen, S., 1995, "Experimental validation of tube-to-support impact computations in cross-flow", Proceedings of 6th International Conference on Flow-Induced Vibration, Bearman, P.W, pp. 383-292.
- Pettigrew, M.J., Sylvestre, Y., Campagna, A.O., 1978, “Vibration analysis of heat exchanger and steam generator designs”, Nuclear Engineering and Design, 48, pp. 97–115.

- Pettigrew, M. J., Goyder, H. G. D., Qiao, Z. L., and Axisa, F., 1986, “Damping of multispan heat exchanger tubes”, ASME PVP, Vol. 104, pp. 81–87.
- Pettigrew, M.J., Taylor, C.E., 1991, “Fluidelastic instability of heat exchanger tube bundles: Review and design recommendations”, ASME Journal of Pressure Vessel Technology, 113, pp. 242–256.
- Pettigrew, M.J., Taylor, C.E., Fisher, N.J., 1998, "Flow-induced vibration: recent findings and open questions”, Nuclear Engineering and Design, 185, pp. 249–276.
- Pettigrew, M.J., Taylor, C.E., 2003, “Vibration analysis of shell-and-tube heat exchangers: an overview, Part 1: flow, damping, fluidelastic instability; Part 2: vibration response, fretting wear, guidelines”, Journal of Fluids and Structures, 18, pp. 469 – 500.
- Polak, D. R., Weaver, D. S., 1995, “Vortex shedding in normal triangular tube arrays”, Journal of Fluids and Structures, 9, 1 – 17.
- Placzek, A., Sigrist, J. F. and Hamdouni, A., 2009, “Numerical simulation of an oscillating cylinder in a cross-flow at low Reynolds number: Forced and free oscillations”, Computers & Fluids, 38, pp. 80–100.
- Price, S. J., 1995, "A review of theoretical models for fluid-elastic instability of cylinder arrays in cross-flow", Journal of Fluids and Structures, Vol. 9, pp. 463-518.
- Rottmann, M., and Popp, K., 2003 “Influence of upstream turbulence on the fluidelastic instability of a parallel triangular tube bundle”, Journal of Fluids and Structures, 18, pp. 595–87.
- Roberts, B. W., 1966, “Low frequency, aeroelastic vibrations in a cascade of cylinders”, Mechanical Engineering Science Monograph, No.4.
- Rogers, R.J., Taylor, C., Pettigrew, M.J., 1984, “Fluid effects on multispan heat exchanger tube vibration”, Proceedings of the ASME Pressure Vessels and Piping Conference, San Antonio, TX, ASME Publication H00316, Topics in Fluid Structure Interaction, pp. 17–26.
- Said, M. N., Mhiri, H., Bournot, H., Le Palec, G., 2008, "Experimental and numerical modeling of the three-dimensional incompressible flow behaviour in the near wake of circular cylinders", Journal of Wind Engineering and Industrial Aerodynamics, 96, pp. 471–502.

- Sasakawa, T., Serizawa, A. and Kawara, Z., 2005, “Fluid-elastic vibration in two-phase cross flow”, Experimental Thermal and Fluid Science, 29, 403–413.
- Sim, W. G., Park, M. Y., 2010, “Fluid-elastic Instability of Normal Square Tube Bundles in Two-Phase Cross Flow”, Proceedings of the 18th International Conference on Nuclear Engineering, May 17- 21, Xi’an, China.
- Simpson, F. J., Hartlen, R. T., 1974, "Wind tunnel determination of fluid-elastic vibration thresholds for typical heat exchanger tube patterns", Ontario Hydro Research Division Report, 74-309-K.
- Singh, K. P., Soler, A. I., 1984, “Mechanical design of heat exchangers and pressure vessel components”, Arcturus Publishers, Cherry Hill.
- So, R.M.C., Wang, X.Q., 2008, “Free-stream turbulence effects on vortex-induced vibration and flow-induced force of an elastic cylinder”, Journal of Fluids and Structures, 24, pp. 481-495.
- Standards of Tubular Exchanger Manufacturers Association, 1988, 7th ed., TEMA, New York.
- Standards of Tubular Exchanger Manufacturers Association, 2007, 9th ed., TEMA, New York.
- Tanaka, H., Takahara, S., 1981, “Fluidelastic vibration of tube array in cross flow”, Journal of Sound and Vibration, 77, pp. 19-37.
- Taylor, C. E., Pettigrew, M. J., 1998, "Vibration damping in multi-span heat exchanger tubes", ASME Journal of Pressure Vessel Technology, 120, pp. 283-289.
- Thulukkanam, K., “Heat Exchanger Design Handbook”, Second edition, CRC Press, Taylor & Francis Group, Boca Raton, Florida.
- Uchiyama, T., 2003, “Numerical prediction of added mass and damping for a cylinder oscillating in confined incompressible gas–liquid two-phase mixture” Nuclear Engineering and Design, 222, pp. 68–78.
- Wambsganss, M.W., Chen, S.S., Jendrzejcyk, J.A., 1974, "Added mass and damping of a vibrating rod in confined viscous fluid" ANL-CT-75-08, Report, Argonne National Laboratory, Argonne, Illinois.
- Weaver, D. S., Grover, L. K., 1978, “Cross-flow induced vibrations in a tube bank - turbulent buffeting and fluid elastic instability”, Journal of Sound and Vibration, 59 (2), pp. 277-294.

- Weaver, D. S., Fitzpatrick, J. A., 1988, “A review of cross-flow induced vibrations in heat exchanger tube arrays”, Journal of Fluids and Structures, 2, pp. 73-93.
- Williamson, C. H. K., Govardhan, R., 2008, “A brief review of recent results in vortex-induced vibrations”, Journal of Wind Engineering and Industrial Aerodynamics, 96, 713 – 735.
- Yahiaoui, T., Adjlout, L., Imine, O., 2010, “Experimental investigation of in-line tube bundles”, Mechanika, 5 (85), pp. 37-43.
- Ziada, S., Oengoeren, A., Buhlmann, E. T., 1989, “On acoustical resonance in tube arrays - Part I: Experiments; Part II: Damping criteria”, Journal of Fluids and Structures, 3, pp. 293 – 324.
- Ziada, S., Oengoeren, A., 1992, “Vorticity shedding and acoustic resonance in an in-line tube bundle - Part I: Vorticity shedding; Part II: Acoustic resonance”, Journal of Fluids and Structures, 6, pp. 271 – 292 and 293 – 309.
- Zdravkovich, M. M., 1977, “Review of the Interference between two circular cylinders in various arrangements”, ASME Journal of Fluids Engineering, 99, pp. 618-633.
- Zukauskas, A. A., 1989, “Vibration of tubes in heat exchangers, in high performance single phase heat exchangers”, Hemisphere, Washington, DC, pp. 316–348.

APPENDICES

Appendix A

Displacement-time Signal from Strain Gauges and Corresponding Fast Fourier Transform (FFT) Plot

At $U_\infty = 3\ m/s$

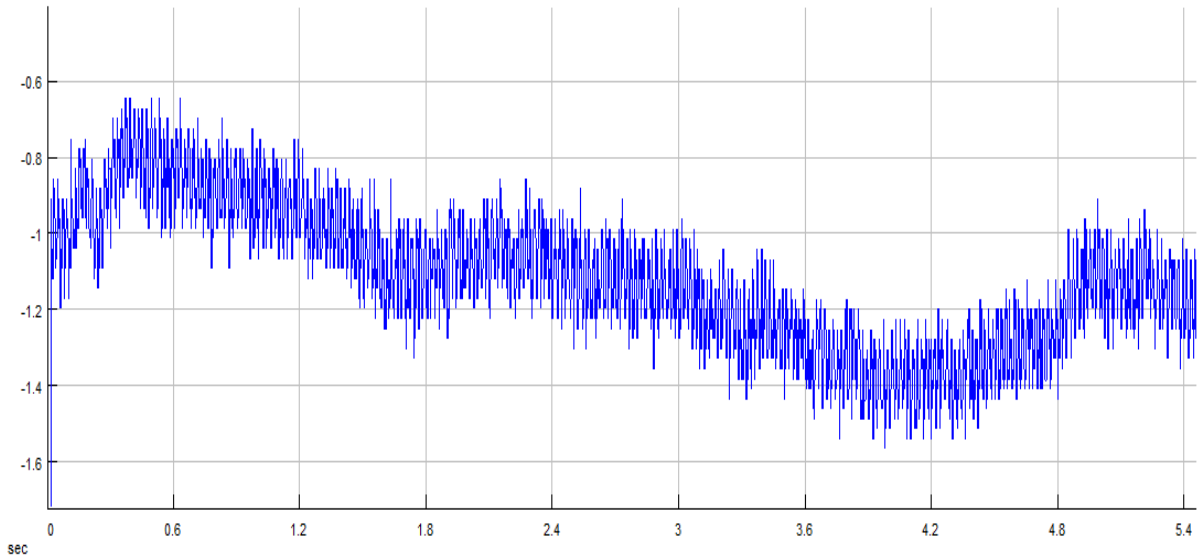

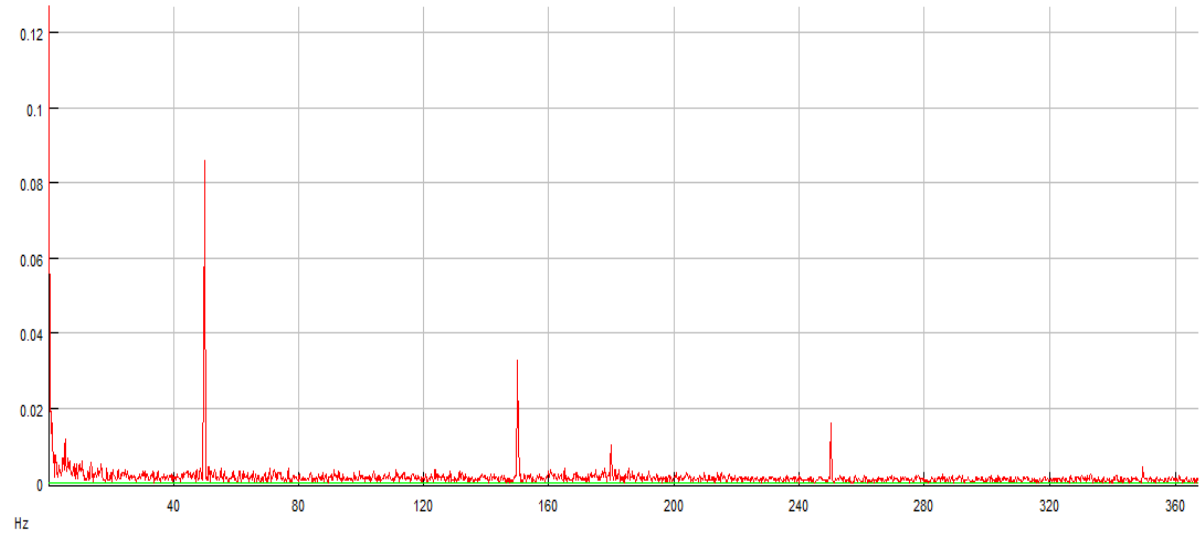

At $U_\infty = 4\ m/s$

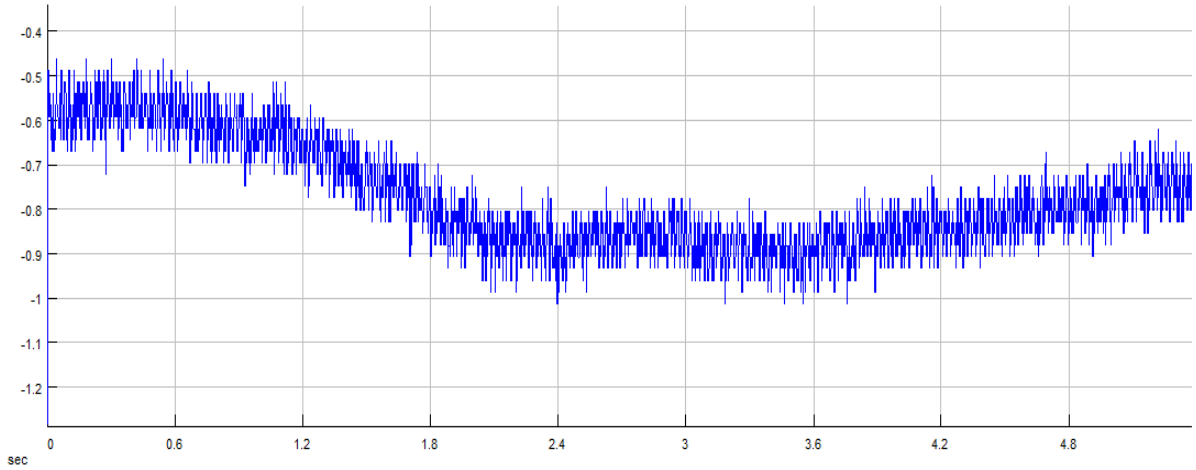

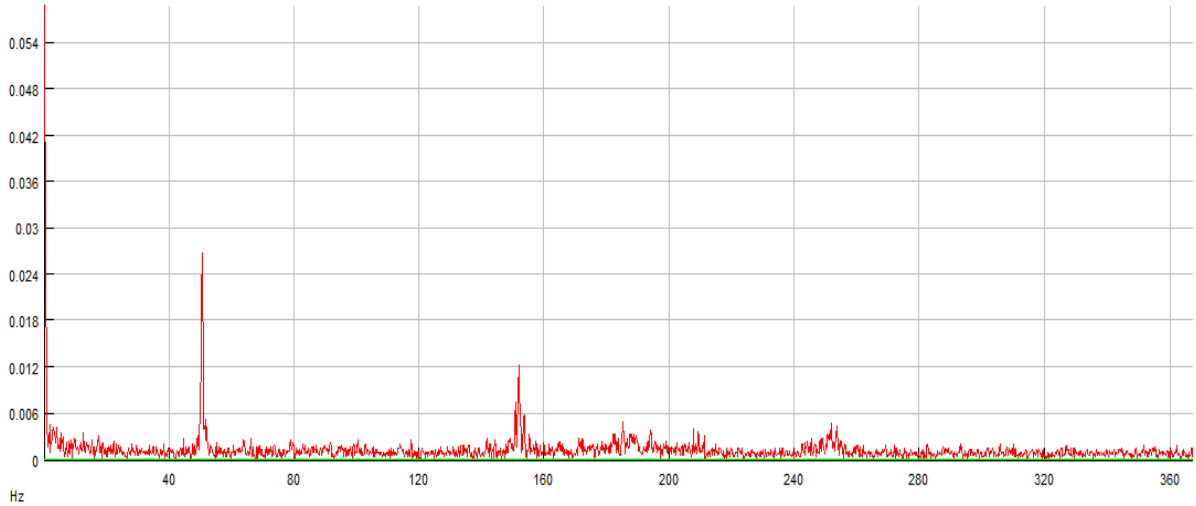

At $U_\infty = 5\ m/s$

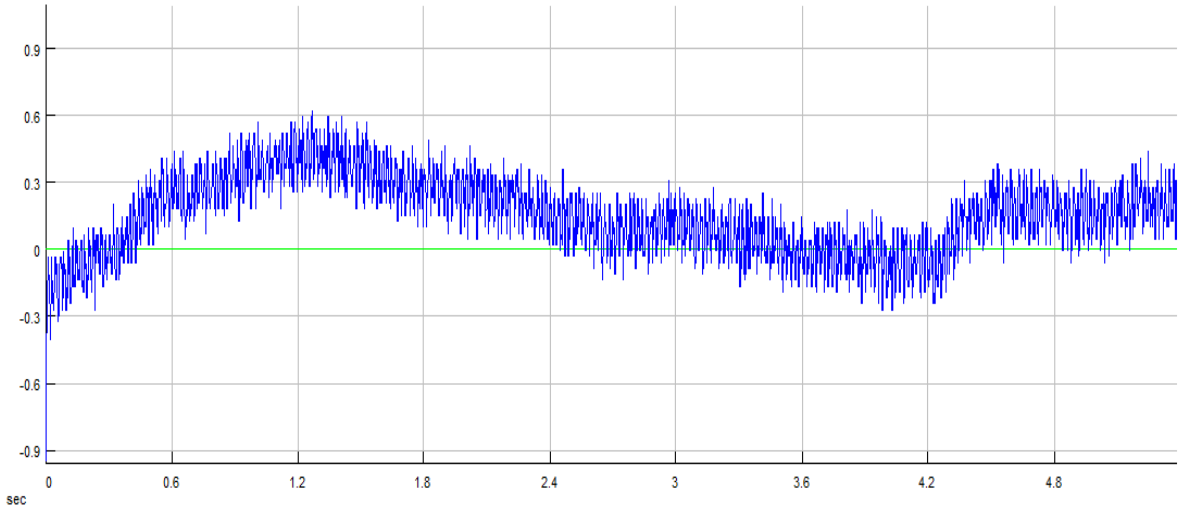

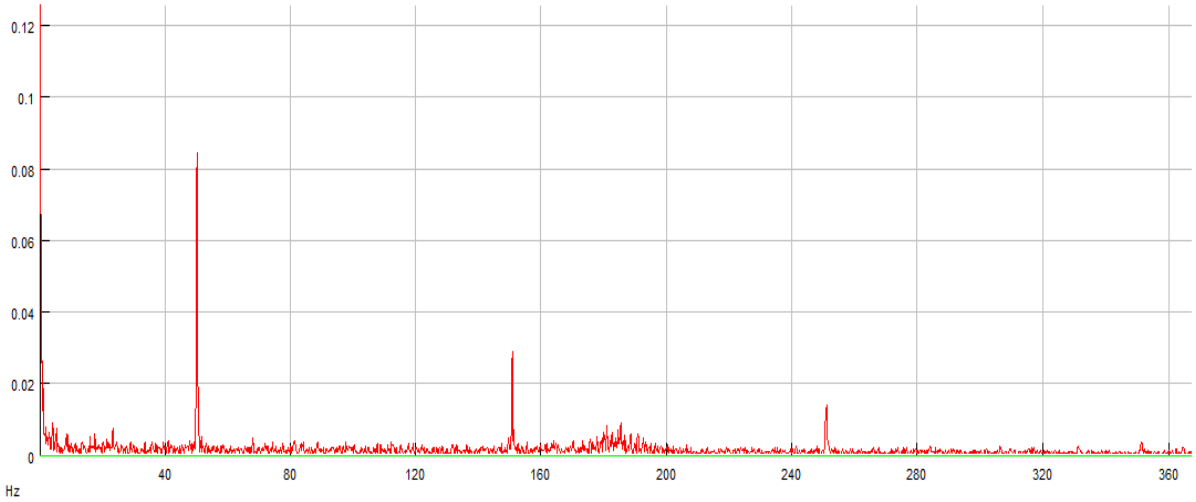

At $U_\infty = 6\, m/s$

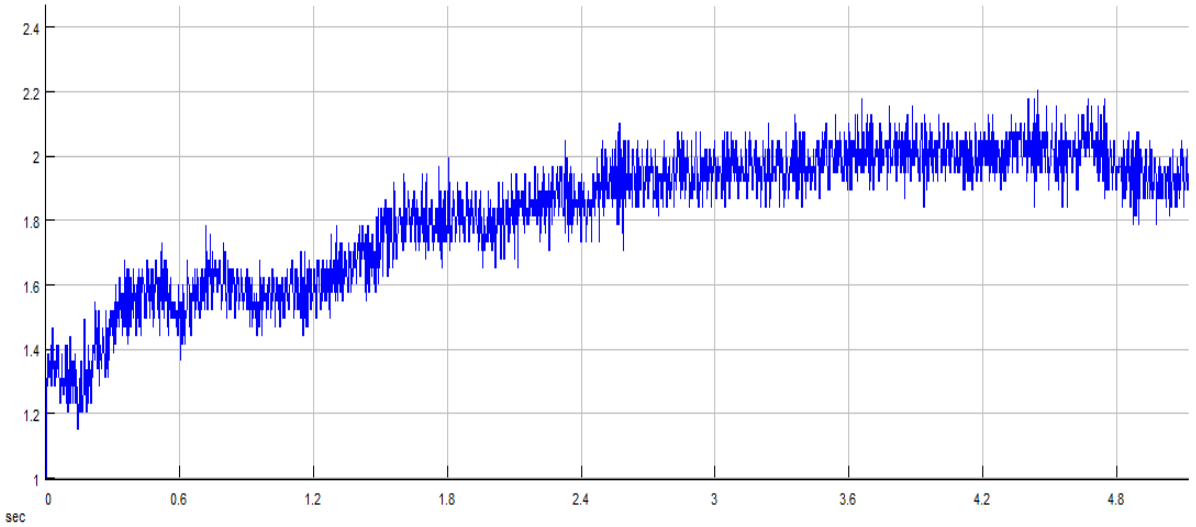

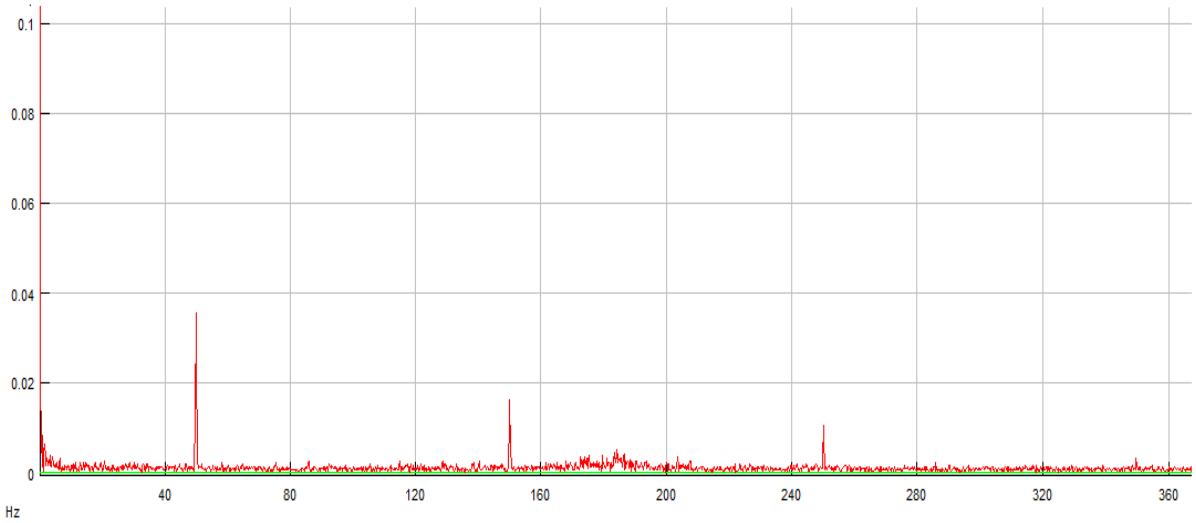

Appendix B

Summary of Experimental Results

Sr. No.	Free stream velocity $U_\infty(m/s)$	Pitch or Gap velocity $U_p(m/s)$	Reduced pitch velocity U_r	RMS Amplitude (mm)		Logarithmic decrement δ		Mass Damping Parameter ($m\delta/\rho D^2$)	
				Flow direction X_{rms}	Lateral direction Y_{rms}	Flow Direction	Lateral Direction	Flow Direction	Lateral Direction
1.	3	9.83	2.26	0.075	0.105	0.005153	0.005283	1.0665	1.0773
2.	4	13.11	3.02	0.086	0.058	0.008992	0.003774	0.8687	0.9854
3.	5	16.38	3.77	0.114	0.116	0.003628	0.005788	0.7302	0.8045
4.	6	19.66	4.53	0.084	0.131	0.005403	0.004533	0.6583	0.7761
5.	7	22.93	5.28	0.109	0.184	0.005550	0.005541	0.6268	0.7166
6.	8	26.21	6.04	0.143	0.158	0.004301	0.006044	0.6112	0.7182
7.	9	29.49	6.79	0.121	0.189	0.003290	0.004535	0.5978	0.7169
8.	10	32.76	7.55	0.149	0.222	0.004556	0.004536	0.5998	0.6865
9.	11	36.04	8.30	0.194	0.218	0.005057	0.005294	0.5653	0.6279
10.	12	39.32	9.06	0.164	0.271	0.003795	0.004284	0.5404	0.6266
11.	13	42.59	9.81	0.187	0.302	0.005556	0.004790	0.5365	0.6572
12.	14	45.87	10.57	0.249	0.345	0.005040	0.007812	0.5367	0.5681
13.	15	49.14	11.32	0.336	0.433	0.005285	0.006042	0.5069	0.5379
14.	16	52.42	12.08	0.489	0.583	0.004523	0.006782	0.5060	0.5381
15.	17	55.70	12.83	0.585	0.635	0.004525	0.008578	0.5102	0.5377
16.	18	58.97	13.59	0.665	0.787	0.004273	0.006797	0.4502	0.5081
17.	19	62.25	14.34	0.798	1.006	0.004266	0.006055	0.4303	0.4477
18.	20	65.53	15.10	0.981	1.149	0.004766	0.006543	0.3903	0.4185